Journal of Molecular Structure 1320 (2025) 139732

Contents lists available at ScienceDirect

Journal of Molecular Structure

journal homepage: www.elsevier.com/locate/molstr

Design and synthesis of new benzothiazole-piperazine derivatives and *in vitro* and *in silico* investigation of their anticancer activity

Asaf Evrim EVREN [a,b,**], Büşra EKSELLİ [c], Leyla YURTTAŞ [a,*], Halide Edip TEMEL [c], Gülşen AKALİN ÇİFTÇİ [c]

[a] Anadolu University, Faculty of Pharmacy, Department of Pharmaceutical Chemistry, 26470, Eskişehir, Turkey
[b] Bilecik Şeyh Edebali University, Vocational School of Health Services, Pharmacy Services, 11000, Bilecik, Turkey
[c] Anadolu University, Faculty of Pharmacy, Department of Biochemistry, 26470, Eskişehir, Turkey

ARTICLE INFO

Keywords:
Benzothiazole
Piperazine
Acetamide
Anticancer activity
Molecular dynamics simulation

ABSTRACT

In this work, novel benzothiazole-piperazine acetamide (**2a-2l**) analogs were synthesized and evaluated their anticancer activity. The ^{1}HNMR , ^{13}CNMR and LC-MS/MS spectral data and elemental analyses were used to clarify the structure of the final molecules. The title compounds were procured by reacting 2-chloro-*N*-(6-substituted benzothiazole-2-yl) acetamide with some piperazine derivatives. Cytotoxicity and apoptosis parameters including Annexin V binding capacities, effect on cell cycle, caspase-3 activation and mitochondrial membrane depolarization effect were evaluated to determine anticancer profile of the final molecules on A549 (human lung adenocarcinoma), C6 (glioma cell line) and NIH/3T3 (mouse embryoblast cell line). Mostly, the final molecules showed significant cytotoxic profile with prominent selectivity. **2c** (IC_{50}: 7.23±1.17, SI: 6.93), **2d** (IC_{50}: 17.50±4.95; SI: 11.59), and 2 h (IC_{50}: 10.83±0.76; SI: 29.23) showed significant and selective cytotoxic activity. Compounds **2b, 2c** and **2e** provoked apoptosis of A549 cells with potential higher than cisplatin as determined by flow cytometry. The cell cycle analysis of 2**b, 2e**, 2 g, and 2 h suggested that the A549 cells were affected during G0/G1 phase. Caspase-3 activation was observed on cells by compounds **2a, 2e, 2i** and **2l** at most. The highest mitochondrial membrane depolarization ratios were seen treated by compounds **2e**, 2 h, and **2j.** None of the analogs displayed any obvious inhibition activity on MMP-9. The physicochemical properties were predicted for all compounds and also molecular docking and dynamics simulation studies were realized for compound **2e,** namely *N*-(6-methoxybenzothiazol-2-yl)-2-(4-(p-tolyl) piperazin-1-yl) acetamide. The results indicated that merging benzothiazole and piperazine derivatives via acetamide bridge is promising in cancer research because these moieties can interact with the loop and ß-sheet regions of MMP-9. So, **2e** was considered as a potential therapeutic agent against lung carcinoma.

1. Introduction

Cancer is described as a group of diseases that are mainly caused by uncontrolled cell division [1]. Lung cancer which is one of the various cancer diseases is the leading cause of cancer death around the world since late diagnosis is the main reason. In more than 40% of cancer cases, patients have already metastasized disease at the time of diagnosis. The treatment using conventional chemotherapeutic agents is rarely successful in long-term survival in this kind of late-stage tumoral disease [2-4]. In fact, the effectiveness of these chemotherapeutic agents is limited by drug resistance. And this challenge is a major restriction against radical treatment of cancer. So, addition to late diagnosis, the drug resistance has become an important issue [5,6]. Although there are some important pharmacological ideas to cancer treatment, the prognosis is poor since the absence of radical treatment and early diagnosis. Therefore, the researchers try to understand the behaviors of resistance mutations of tumor cells and focus on the synthesis of new compound to apply on pathways such as apoptosis [7-14]. Caspases are activated to trigger apoptosis, which causes several biological processes, like cell cycle regulation and signaling pathways. On the other hand, in addition to that, these activations are also related to the morphological manifestations of apoptosis, such as DNA condensation and fragmentation,

* Corresponding author.
** Corresponding author at: Anadolu University, Faculty of Pharmacy, Department of Pharmaceutical Chemistry, 26470, Eskişehir, Turkey.
E-mail addresses: asafevrimevren@anadolu.edu.tr, asafevrim.evren@bilecik.edu.tr (A.E. EVREN), lyurttas@anadolu.edu.tr (L. YURTTAŞ).

https://doi.org/10.1016/j.molstruc.2024.139732
Received 12 May 2024; Received in revised form 5 August 2024; Accepted 20 August 2024
Available online 22 August 2024

and membrane blebbing [15,16]. Matrix metalloproteinase-9 (MMP-9) is another enzyme which is one of the markers of disease that is over-expressed in cancerous cells. MMP-9 inhibition is considered noteworthy approach for blocking tumor promotion and metastasis [17].

Benzothiazole and its derivatives are versatile ring systems in terms of their biological activity. The scaffold occurs in many classes of biologically active compounds such as antimicrobial [18,19], antiviral [20], antimalarial [21], anti-Alzheimer's disease [22], anti-neuropsychiatric [23], neuroleptic [24], antinociceptive [25] agents. Therewithal, benzothiazole moiety is founded in many anticancer compounds [26,27]. Specifically, they showed their selective inhibitory activity against cancer cells [28-33].

Literature review inspired that piperazine derivatives have several biological activity such as antimicrobial [34,35], antiviral [36], analgesic [37] and antidepressant [38]. Because of their selective inhibitory activity against cancer cells [39-41] and their key role in many anticancer compounds [42], they have gained an important status in medicinal chemistry, especially, from the point of view of anti-lung cancer activity [43-45]. Imatinib and Dasatinib, which contain a piperazine moiety, are two good examples of anticancer drugs.

In our previous work, we reported that *N*-(substituted phenyl) piperazine moieties [46,47] and *N*-(6-methyl/methoxy/ethoxy benzothiazole) acetamide derivatives [48] displayed potent cytotoxic activities. That's why, our designing process was formed around the hybridization of the structures of previous works. On the other hand, there are many studies reported about the constitution of novel anticancer ligands that have specific features, and also these were investigated via *in silico* methods, then they were reported [49-54]. So, an acetamide bridge was used to link benzothiazole and piperazine rings as shown Scheme 1. Additionally, some studies have reported the importance of benzothiazole-piperazine hybrids [55,56]. These reports indicated that these two ring systems act synergistically, positively affecting the anticancer effect profile. In our design, we expect similar synergism.

According to the above information, twelve novel benzothiazole-bearing piperazine analogs were designed, and synthesized, and then their purification and characterization were reported. According to the design proposal, the anticancer activity profile was tested via *in vitro* studies, then considering *in vitro* studies, active molecules were also investigated via *in silico* studies, finally, all results were used to explain the substituent effects on anticancer profile.

2. Results and discussion

2.1. Chemistry

In this study, twelve new compounds containing benzothiazole and piperazine rings linked by an acetamide bridge as a core structure were synthesized. The final molecules were obtained by two steps. Firstly, 6-substituted benzothiazole derivatives were acetylated with chloroacetyl chloride. At last step, the media product 2-chloro-*N*-(6- substituted benzothiazole) acetamide analogs (**1**) and 4-substituted piperazines were reacted and produced *N*-(6-substituted benzothiazole-2-yl)−2-(4-substituted piperazin-1-yl)acetamides (**2a-2l**) as displayed in Scheme 2. The structural analyzed of the final compounds were done by analytical and spectral data (**Figs. S1-S28**). Some characteristic properties of the synthesized compounds (**2a-2l**) were shown in Table 1.

The ^{1}HNMR spectra of compounds showed signals at δ 3.38–3.94 ppm (CH_2) for acetyl protons which were singlet peaks. Piperazine protons were observed at δ 2.67–3.17 ppm (CH_2) as broad singlet peaks. The signals seen at δ 10.94–12.60 ppm indicated the acetamide N—H proton. The peaks observed as a pair of singlets, doublets, triplets and/or multiplets at δ 6.79–9.60 ppm were the aromatic protons of the aromatic rings. The ^{13}CNMR spectra of compounds showed signals at δ 60.45–60.68 ppm for methylene carbon (CH_2), at δ 48.42–53.01 ppm for piperazine's methylene carbon (CH_2), at δ 105.18–163.62 ppm for aromatic carbon and at δ 169.45–170.62 for carbonyl (C=O) carbon. *M* + 1 peaks in LC-MS/MS spectra were in agreement with the calculated molecular weight of the target compounds (**2a-2l**). Elemental analysis

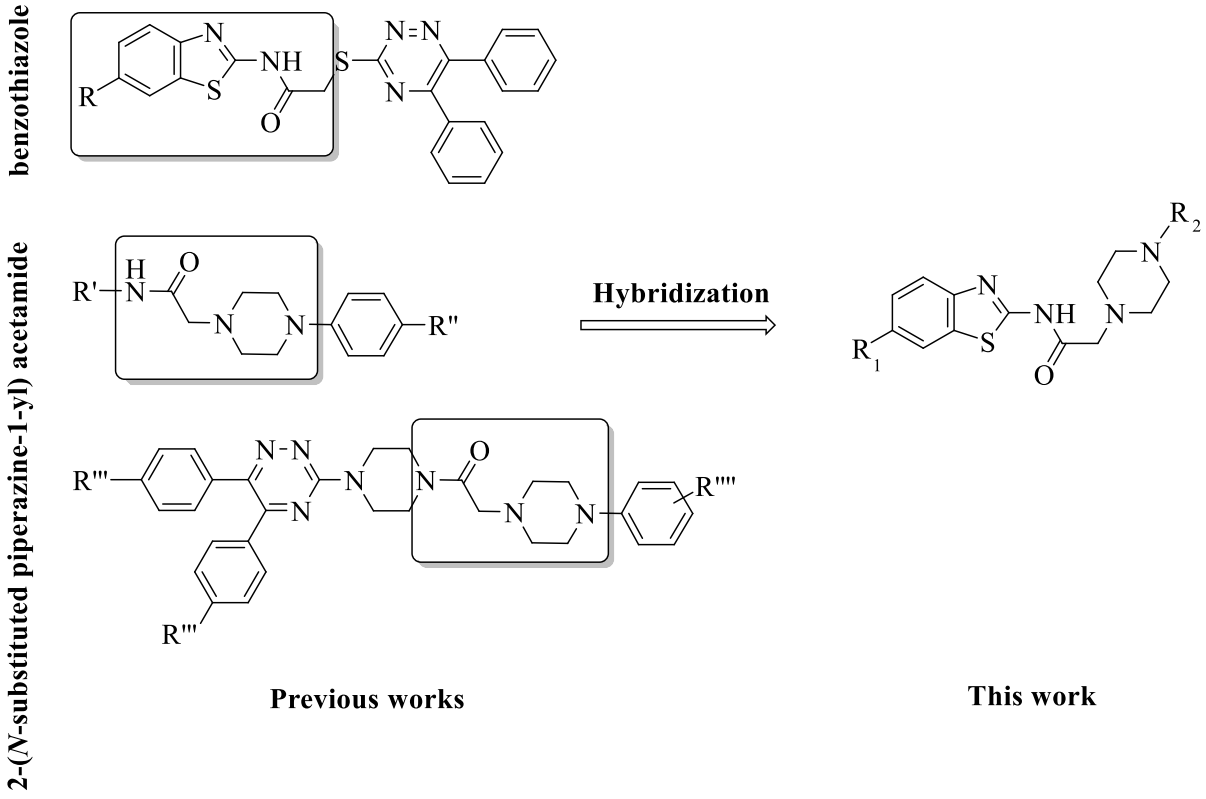

Scheme 1. Designed strategy of benzothiazole-piperazine compounds.

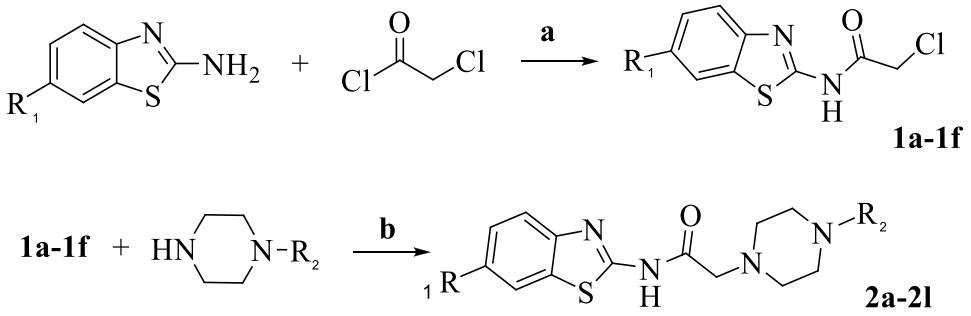

Scheme 2. General procedure for the synthesis of the compounds. Reactions & Conditions: a) THF, TEA, 0 °C, after dropping, rt 4 h; b) THF, TEA, 2 h, rt.

Table 1
Synthesized compounds (**2a-2l**).

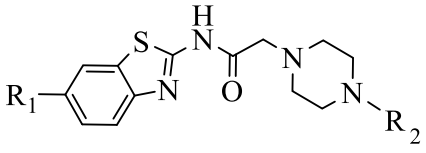

Compound	R_1	R_2	Compound	R_1	R_2
2a	-F	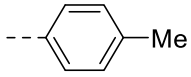	**2g**	-Me	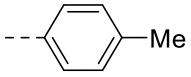
2b	-F	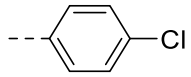	**2h**	-Me	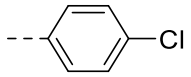
2c	-	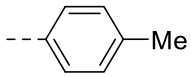	**2i**	-OEt	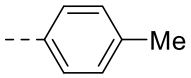
2d	-	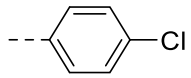	**2j**	-OEt	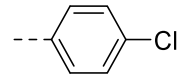
2e	-OMe	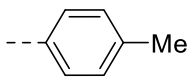	**2k**	$-NO_2$	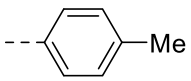
2f	-OMe	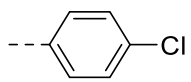	**2l**	$-NO_2$	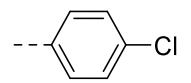

results for C, H, and N elements were acceptable with calculated values of the compounds. HPLC indicated that the purity of the most active compounds (**2b, 2e**, 2 g and 2 h) were 94.836%, 96.165%, 96.640% and 90.311%, respectively.

2.2. Anticancer activity

2.2.1. Cytotoxicity

To find new cytotoxic agents against cancer cells, the most preferable methods are the screening test compounds against a panel of different cancer and healthy cell lines. The cytotoxicity assays and determination of IC_{50} doses of standard drug, cisplatin, and final compounds against A549, C6 and NIH/3T3 cell lines were performed by MTT assay, in this study. The formazan formation was quantified spectrophotometrically at 540 nm using a microplate reader.

The results indicated that cisplatin IC_{50} value was indicated 35.55 ±5.09 μM against A549 cells, and the most active compounds were stated **2b,** 2 g and 2 h (IC_{50}: <9.65 μM, <10.28 μM and <9.77 μM, respectively). In addition, IC_{50} values of compounds **2a, 2c, 2e, 2f, 2i, 2j** and **2l** were lower than IC_{50} values of cisplatin against A549 cells, so it means that the synthesized compounds were more active than cisplatin at the same concentrations, excluding compounds **2d** and **2k**. Anticancer activity of the compounds **2d** and **2k** was found so low in comparison to cisplatin. Moreover, according to IC_{50} values that was determined against NIH/3T3 cells, all compounds showed a non-cytotoxic profile at the IC_{50} values that were applied to A549 cells, except compound **2l** Additionally, the selectivity index (SI) of the synthesized compounds was calculated. The calculation displayed that compound **2e,** 2 g and 2 h were highly selective on A549 cells (SI= >33.96, >23.03, and >32.40, respectively). On the other hand, except **2d** and **2l** (SI=1.18 and 1.23), compounds showed affinity on lung cancer cells rather than healthy cells. Meanwhile, except compound **2a** (IC_{50}: >500 μM), all compounds showed cytotoxicity on C6 glioma cells. Compounds **2c** (IC_{50}: 7.23±1.17 μM), **2d** (IC_{50}: 17.50±4.95 μM), 2 h (IC_{50}: 10.83±0.76 μM), and **2j** (IC_{50}: 11.83±0.29 μM) have comparable cytotoxic activity to cisplatin, and their SI values were calculated as 6.93, 11.59, 29.23, and 2.36, respectively. Also, compounds **2e** (>16.86 times) and **2k** (>34.69 times) have very high selective anti-glioma activity than cytotoxicity on healthy cells. All findings are shown in Table 2.

After determination of the most effective compounds against both cancer cells with low cytotoxicity against NIH/3T3 cells, the apoptotic effects of final products and reference drug were tested according to Annexin V- PI binding capacities in flow cytometry method. The results show that the apoptotic death percentage of cancer cells was higher than the necrotic death percentage for all final compounds, except compounds 2 g. Following flow cytometric analyses, the early and late apoptotic effects of compounds **2a, 2b, 2c, 2e, 2f,** 2 g, 2 h, **2j, 2k** and **2l** (for IC_{50} doses) on A549 cell line were determined as 12.4%, 17.1%, 18%, 20.9%, 12.4%, 6.5%, 7.2% and 15.8%, while their viabilities were determined as 84.6%, 70.4%, 79.4%, 73.7%, 80.6%, 90.9%, 88.4% and 78.3%, respectively. According to these findings, compounds **2b, 2c** and **2e** showed higher apoptotic effects on A549 cells compared to cisplatin (16.0%) In fact, compounds **2b, 2f, 2j**, and **2k** have killed the cancer cells via apoptotic pathway, but they also got a higher rate of necrotic pathway. Compounds **2a, 2c, 2e,** 2 h and **2l** were in comparison with compounds **2b, 2f, 2j**, and **2k**, have significantly killed A549 cancer cells via the apoptosis. Especially, compounds **2c, 2e**, and **2l** have significantly higher apoptotic percentages than their necrotic percentages. These results are shown in Fig. 1 and Table 3 as percentages.

Table 2
IC_{50} values of the tested compounds against A549, C6 and NIH/3T3 cell lines (μM).

Comp.	NIH/3T3 (IC_{50})	A549 (IC_{50})	S.I.	C6 (IC_{50})	S.I.
2a	77.23±9.14	22.74±3.70	3.40	>500	<0.16
2b	29.28±17.77	<9.65	>3.03	21.83±5.80	1.34
2c	50.07±7.88	16.66±0.47	3.01	7.23±1.17	6.93
2d	202.88±26.96	172.67 ±26.96	1.18	17.50±4.95	11.59
2e	>1000	29.45±3.86	>33.96	59.33±11.02	>16.86
2f	29.64±1.39	10.65±0.77	2.78	112.33 ±28.57	0.26
2 g	236.74±26.30	<10.28	>23.03	33.50±12.02	7.07
2h	316.58±62.90	<9.77	>32.40	10.83±0.76	29.23
2i	97.52±12.19	19.59±1.23	4.98	36.33±7.51	2.68
2j	27.90±4.65	10.08±0.36	2.77	11.83±0.29	2.36
2k	>1000	149.99±3.72	>6.67	25.83±6.21	>34.69
2l	15.47±3.55	12.60±1.19	1.23	43.75±1.77	0.35
R.D.	N.T.	35.55±5.09	N.C.	19.50±0.71	N.C.

R.D.: Reference Drug (cisplatin). The IC_{50} values were reported as the average of three independent determinations and its unit is μM. **N.T.:** not tested; **N.C.**: Not calculated. **S.I.**: Selectivity index calculated by following formula (S.I.: IC_{50} on normal cells/IC_{50} on cancer cells).

2.2.2. Activation of caspase-3 enzyme

Caspase-3, which is found in the middle of extrinsic and intrinsic pathway is a key enzyme in the initiation of cellular events during early apoptotic process. The results of caspase-3 enzyme activity positive (+) cells showed that compounds **2e** (40.5%), **2i** (34.4%) and **2l** (32.1%) have notable stimulation the enzyme activity as can be seen on Fig. 2 and Table 4. Also, caspase-3 activity positive (+) cells percent for cisplatin was determined as 57.9. Previous reports about caspase-3 inhibition activity [59,60] indicated that 6-methoxybenzothiazole cores have great potential. The results revealed that **2e** (methoxy) and **2i** (ethoxy), the most active compounds, showed similar potential in the activation of the caspase-3 enzyme allosterically.

2.2.3. Mitochondrial membrane depolarization

Identifying the changes in the mitochondrial membrane potential (MMP) is one of the hallmarks of apoptosis. In order to investigate the changes on MMP of the effects of compounds **2a, 2b, 2c, 2e, 2f**, 2 g, 2 h, **2j, 2k** and **2l** on A549 cells, these cells were incubated by the IC_{50} concentrations of above compounds for 24 h. The depolarization of the membrane potential of the compounds **2e** (19.7%), 2 h (41.2%), and **2j** (28.3%) was remarkable, especially, since their values were higher than cisplatin (14.2%) as shown in Fig. 3 and Table 5. Therefore, these compounds caused higher disturbance on mitochondrial membrane potential in A549 cells and that were marked as effective and may be considered for the next drug design studies.

2.2.4. Cell cycle analysis

In this study, 24-hour life cycles of A549 cells treated with three analogs (**2b, 2e**, 2 g, and 2 h) that have the lowest IC_{50} value were chosen to investigate piperazine-benzothiazole hybrid effects on cell cycle were analyzed by flow cytometry. The results are displayed in Table 6 and Fig. 4. Compounds **2b, 2e,** 2 g, and 2 h have impact selectively on G_0/G_1 phase rather than S and G2/M phases which is a preferred and desirable feature for antitumoral agents. The results also indicated that the major effect was made by 6-florobenzothiazole and 4-chlorophenyl piperazine hybrid, however, both 6-methylbenzothiazol analogs (4-methylphenyl and 4-chlorophenyl piperazines) are also found effective. In fact, in previous studies [57,58], small substitution on benzothiazole were suggested to reach desirable effects on cell cycles, so, since our results also displayed similar results, we support these suggestions.

2.2.5. MMP-9 inhibition

The inhibition percentages of standard agent, NNGH (positive control), and the compounds **2e** and **2f** were determined as 91.59±0.68, 46.36±2.12, and 48.56±1.80, respectively. On the other hand, the inhibition activity of other compounds was not higher than 40% (Table 7). In fact, these results have been frustrating because we previously reached 6-methyl and 6-florobenzothiazole analogs [58] that showed

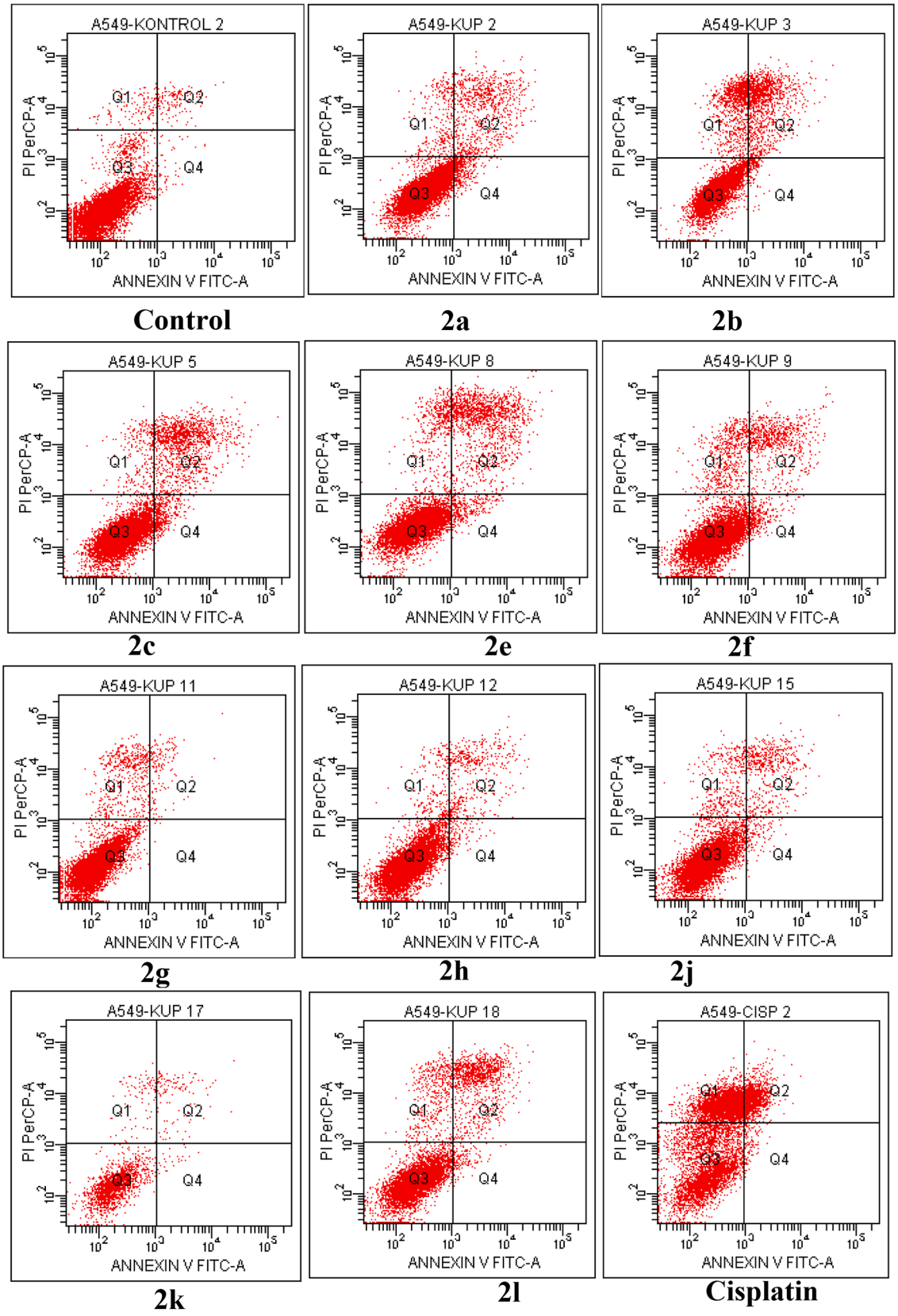

Fig. 1. Flow cytometric analysis of A549 cells treated with IC_{50} values of compounds 2a, 2b, 2c, 2e, 2f, 2 g, 2 h, 2j, 2k, 2l and cisplatin. At least 10.000 cells were analyzed per sample, and quadrant analysis was performed.

Table 3
Apoptotic rates of synthesized compounds on A549 cell lines.

	Q1	Q2	Q3	Q4	Q2+Q4
2a	3.0	8.7	84.6	3.7	12.4
2b	12.5	15.6	70.4	1.5	17.1
2c	2.6	14.1	79.4	3.9	18.0
2e	5.4	17.5	73.7	3.4	20.9
2f	6.9	8.9	80.6	3.5	12.4
2 g	5.4	1.6	93.0	0.1	2.7
2h	2.6	5.1	90.9	1.4	6.5
2j	4.3	5.9	88.4	1.3	7.2
2k	4.5	5.4	88.8	1.3	6.7
2l	5.9	14	78.3	1.8	15.8
Control	1.4	1.5	96.7	0.5	2.0
R.D.	42.7	15.0	41.3	1.0	16.0

Q1: Necrotic cells, **Q2**: Late apoptotic cells, **Q3**: Viable cells, **Q4**: Early apoptotic cells, **Q2**+**Q4**: Early and late apoptotic cells. **R.D.:** Reference drug (Cisplatin).

great affinity to the MMP-9 enzyme. To get more information, we benefited from *in silico* studies for the relation between these compounds and the MMP-9 enzyme.

2.3. Prediction of ADME parameters and druglikeness rules

One of the important drug availability parameters is the pharmacokinetic features of the drug-candidate compounds. In particular, some preliminary tests such as the determination of absorption, distribution, metabolism, excretion (ADME) features are very important due to the occurrence of novel molecules resulting from the original compound synthesis studies that accelerated at the end of the 1990s. So, after identification these features of the new compounds, relationship between molecular structure and their properties can be worked up a connection [61-65].

Molecular weights were calculated between 366.15–431.08. Log P values which indicate partition factor were found between 4.04–76. Drug-likeness model scores (DLMS) were found between 0.12 and 1.22. The number of hydrogen bond donor (HBD) was stated as 1 for all compounds. Also, the number of hydrogen bond acceptor (HBA) was determined as 8 for **2k** and **2l**, as 5 for compounds **2a-2d**, 2 g and 2 h and as 6 for rest of them. Molecular volume was calculated between 329.66–375.03 A^3. Topological polar surface area (TPSA) was determined between 48.47 and 94.29. When all the findings were examined, it was determined that there was no violation according to Lipinski's rule of five. Therefore, according to ADME prediction, all compounds can be used oral. Even if there is no exact finding in practice, these scores are in harmony highly with the activity potential of the compounds. Additionally, all final molecules were appropriative according to druglikeness rules. As a last, final compounds can pass blood-brain barrier except **2e, 2f, 2i, 2j, 2k**, and **2l**, thus, compounds **2a-2d**, 2 g and 2 h can be used in the treatment of brain cancer. All findings were shown in Table 8.

2.4. In silico studies

The experimental results were consulted to investigate the binding modes via the molecular docking procedure. Due to the experimental results, compounds **2b** and **2e** among selective compounds have similar apoptotic effects to the standard drug, cisplatin, while only compound **2e** showed a similar caspase-3 effect to the standard agent. Also, compound **2e** has more potential than its analogs for MMP-9 inhibition activity. Therefore, our research group focused on compound **2e** to recognize the binding modes of proteins-piperazine derivatives, meanwhile, we wanted to clarify the structure-activity relationship and performed the molecular docking study. The best docking poses of compound **2e** were showed in Figs. 5-10.

2.4.1. Molecular docking studies on caspase-3 enzyme

Compound **2e** built up H-bonds with Arg64, Ser205, and Arg207, also interacted with Hip121 (salt bridge) and Tyr204 (π- π stacking) at allosteric form of caspase-3 active site (PDBID: 4EHA). On the other hand, it connected with Arg64, Hie121 and Arg207 via H-bonds at caspase-3 active site (PDBID: 4QTX). For the both type of caspase-3, compound **2e** had interaction with the important catalytic residue His121.

2.4.2. Molecular docking studies on MMP-9 enzyme

Matrix metalloproteinase (MMP) is a class of Zinc ions-dependent proteolytic enzyme that plays an important role in cancer research. Since the interactions between histidine (226, 230, and 236) and the divalent metal ion (Zn) are important, interactions with these residues should be observed if the ligand is showing inhibition. According to results, compound **2e** connected with His230 (π- π stacking) and Zn301 (salt bridge). Additionally, it showed interactions with Leu188 (H-bond), Glu227 (salt bridge), and Tyr248 (π- π stacking).

2.4.3. Molecular dynamics simulation study on MMP-9 binding pocket

The system stability was evaluated according to **Fig. S29**. As stated in literature [62,66-68], the stability plots indicated that the system protected its stability during the entire simulation time. Because of that, the interaction plots (Fig. 11) and **video** were examined from the simulation's beginning to end. The interactions were observed as H-bonds (sequence number: 188, 189), water-mediated H-bonds (seq. 186, 187, 188, 189, 190, and 227), aromatic H-bonds (seq. 192, 222, 236, 242, 243, 245, 246, 247, 249), ionic (seq. 227), and hydrophobic contacts (seq. 187, 190, 223, 226, 247, and 248). The interactions with Gly186, Leu187, Ala189, His226, and Tyr248 were observed frequently, therefore, we suggested that these interactions supported the system stability. Most importantly, the interactions with Leu188 and Ala190 residues have a major impact on inhibitory activity because of their continuous. Therefore, among all contacts with the loop (seq. 172–188 and seq. 192–201) and ß-sheet (seq. 189–191) residues, the interactions with Leu188 and Ala190 residues play a key role in binding to active region. On the other hand, the *N*-(4-methylphenyl)piperazine moiety fit well the pocket of the binding site, and its phenyl ring frequently interacted with His 226, one of the metal binding residues while its protonated nitrogen (N_1) of piperazine occasionally interacted with Glu227, making a salt bridge with the metal ion. However, after 2.15 ns from the beginning, 2e did not directly contact the Zn ion, it is probably caused by the water molecules (environmental effects), because they mediated interactions with ß-sheet amino acids (seq. 189–191). All these data clarified the possible binding mode of benzothiazole-piperazine hybrids to stabilize the MMP-9 enzyme. In a result, the MDS analysis supported and clarified the docking study at three points:

1) The acetamide bridge is important in inhibitory activity as it binds to ß-sheet and stabilizes the system. It increased the stability of MMP-9 inactive form as expected.
2) The benzothiazole moiety faced the metal binding region and made a hydrophobic balloon that blocked the catalytic pocket against water molecules. Even though blocking, the absence of metal coordination interactions results in a moderate inhibition effect.
3) The piperazine moiety fit well into the active pocket and was binding to Zn-binding histidine amino acids (in this case His226). These interactions were fundamental as they stabilized the active pocket's loop region.

2.5. Substituents effects on anticancer activity

Both findings obtained by *in vitro* and *in silico* were indicated that 6-methoxybenzothiazol moiety (**2e, 2f**) was found more favorable starting structure than the others. Although 6-ethoxybenzothiazoles (**2i, 2j**) showed good activity against A549 cells at low doses, it paled in

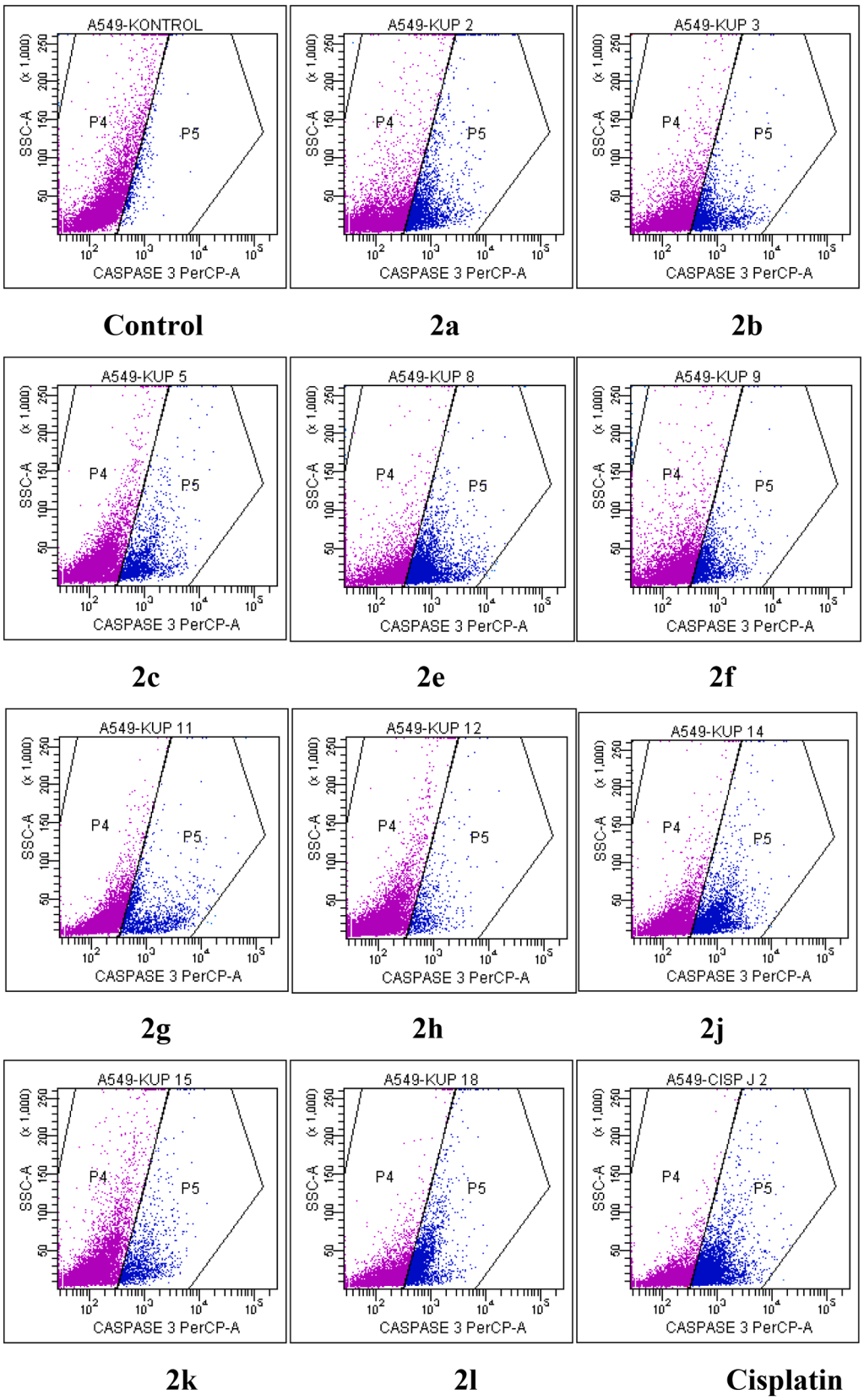

Fig. 2. Caspase-3 activity results after 24 h incubation of A549 cells with compounds **2a, 2b, 2c, 2e, 2f,** 2 g, 2 h, **2j, 2k, 2l** and cisplatin.

Table 4
Percent of quadrant analysis of active Caspase-3 phycoerythrin staining by flow cytometry of A549 cells treated with IC_{50} of the compounds.

Comp.	(+)%	(-)%	Comp.	(+)%	(-)%
2a	27.1	74.6	**2 g**	14.4	86.2
2b	17.8	83.4	**2h**	5.9	94.4
2c	17.5	83.0	**2i**	34.4	66.6
2e	40.5	61.4	**2j**	12.0	88.4
2f	17.0	83.7	**2l**	32.1	70.6
Control	3.1	97.2	**R.D.**	57.9	44.1

R.D: Reference Drug (cisplatin), **(+)%**Caspase-3 activity positive (+) cells (%) and **(-)%:** Caspase-3 activity negative (-) cells.

comparison to its methoxy analog as it did not kill the cancer cells apoptotic way and the MMP inhibition power was weak. Likewise, although 6-methylbenzothiazoles (2 g, 2 h) showed high activity against A549 cells at low doses and had high selectivity on cancer cells, they were also not favorable since the death of cells did not occur via the apoptotic way.

On the other hand, 6-flourobenzothiazoles (**2a, 2b**) showed anticancer activity against A549 and had a good caspase-3 activity profile. However, their MMP inhibition was not sufficient. Therefore, the anticancer activity of these two compounds was not through the MMP-9 pathway, but through another cancer pathway was reported in this study. For this reason, our research will continue to determine the pathway on these two molecules for further studies.

Non-substituted benzothiazoles (**2c, 2d**) were found active yet **2d** had a bad SI profile. Even though compound **2c** acted through the apoptotic way, unfortunately, its inhibition activity on MMP-9 was lower than 40%, thus, **2c** went by the wayside.

Although compound **2k** (6-nitrobenzothiazole derivative) did not display cytotoxicity on healthy cells, its IC_{50} value on A549 cells was calculated higher than others. That's why the compound **2k** was not marked as a desirable candidate for the anticancer activity. However, compound **2l** (6-nitrobenzothiazole) had a low IC_{50} value but its selectivity index was almost 1 which means not acceptable for the candidature to the potential drugs.

From another perspective, generally, the 4-methylphenyl piperazines were found slightly more active than the 4-chlorophenyl piperazines. But there were no differences for IC_{50} values to determine which one was better than the other. On the other hand, there were significant differences in the caspase-3 enzyme activity and mitochondrial membrane polarization. Results indicated that 4-methylphenyl piperazine derivatives positively stimulate the caspase-3 enzyme activity more than the 4-chlorophenyl piperazine derivatives, in contrary to that, 4-chlorophenyl piperazine analogs depolarized the mitochondrial membrane potential more than them. Eventually, apoptotic cell death is controlled by two mechanisms: the extrinsic death receptor pathway and the intrinsic mitochondrial pathway. However, both pathways converge at caspase-3 [69]. In conclusion, 4-methylphenyl piperazines were found more acceptable since the result of caspase-3 is the common pathway. But also, no matter which pathway proceeds to obtain apoptotic death, it will be clarified and expand the SAR studies of the 4-chlorophenyl piperazine derivatives on apoptosis in future studies.

The results suggested that if the benzothiazole has a small, electron-donating substitution (methoxy, methyl) and links with 4-methylphenyl piperazine, the anticancer activity profile was more ambitious. Also, using the acetamide bridge to link the ring systems was proved itself once more as important for the activity [49,70,71].

3. Conclusion

We designed and synthesized new benzothiazole-piperazine derivatives and tested their cytotoxicity profiles against A549 lung carcinoma, C6 glioma and NIH/3T3 cell lines. Meanwhile, some anticancer features such as inducing apoptosis, effect on the cell cycle, effect on the caspase-3 enzyme, effect on the mitochondrial membrane, and inhibition effect on MMP-9 enzyme, of the active compounds were investigated. Mostly, final compounds displayed potent inhibitory effects on A549 and C6 cell lines. In particular, compound **2e** was identified as the most promising apoptosis inducing agent due to its significant apoptotic effects on A549 cell line. It increased caspase-3 cell population and showed significant mitochondrial membrane depolarization activity more than cisplatin. Moreover, molecular docking and molecular dynamics simulation studies were run to understand the binding mode with the target proteins using compound **2e** as a model. *In vitro* and *in silico* studies were in harmony and suggested that compound **2e** stands out as a promising anticancer drug candidate for further *in vivo* studies. Briefly, our study set forth compound **2e** that could be useful as an anticancer agent. Also, it can be concluded similar compounds may display their anticancer activity by acting on apoptotic pathways.

4. Materials and methods

4.1. Chemistry

All chemicals were purchased from Sigma-Aldrich Chemical Co (Sigma-Aldrich Corp., St. Louis, MO, USA) and Merck Chemicals (Merck KGaA, Darmstadt, Germany). All melting points (m.p.) were determined by MP90 digital melting point apparatus (Mettler Toledo, Ohio, USA) and were uncorrected. All reactions were monitored by thin-layer chromatography (TLC) using Silica Gel 60 F254 TLC plates (Merck KGaA, Darmstadt, Germany). Spectroscopic data were recorded with the following instruments: ^{1}HNMR (nuclear magnetic resonance) Bruker DPX- 300 FT-NMR spectrometer, ^{13}CNMR , Bruker DPX 75 MHz spectrometer (Bruker Bioscience, Billerica, MA, USA); $M + 1$ peaks were determined by Shimadzu 8040 LC/MS/MS system (Shimadzu, Tokyo, Japan). Elemental analyses were performed on a Leco 932 CHNS analyzer (Leco, Michigan, USA).

4.1.1. General procedure for the synthesis of the N-(substituted benzothiazol-2-yl)−2-chloroacetamide derivatives (1a-1f)

In a bottom flask, *N*-(substituted benzothiazol-2-yl)−2-amine (1 eq.) and triethylamine (1.2 eq.) were added and dissolved in THF with a constant stirring at 0–5 °C. After cooling, diluted chloroacetyl chloride (1.5 eq.) in THF was added dropwise gradually to this solution. The reaction mixture thus obtained was further agitated for 4 h at room temperature. After the solvent was vaporized to dryness, the solid was washed with water and filtered. After that, raw product was recrystallized from ethanol.

4.1.2. N-(6-substituted benzothiazole-2-yl)−2-(4-substituted piperazin-1-yl) acetamide derivatives (2a-2l)

In a bottom flask, *N*-(6-substituted benzothiazol-2-yl)−2-chloroacetamide (1 eq), and piperazine derivatives (1 eq) were added in THF, then triethylamine (1.2 eq) was added into this mixture to dissolve the solid phase. The reaction thus acquired was further agitated for 2 h at room temperature. The completion of the reaction was controlled by TLC, and after the solvent was evaporated to dryness, the solid was washed with water and filtered. After that, crude product was recrystallized from ethanol. The chemical properties were given in Table 1.

4.1.3. N-(6-fluorobenzothiazol-2-yl)−2-(4-(p-tolyl) piperazin-1-yl) acetamide (2a)

Brown solid, yield 80%, m. p. 125 °C, ^{1}HNMR (300 MHz, DMSO-d_6, ppm) δ 2.19 (s, 3H, CH_3), 2.68 (brs, 4H, piperazine-CH_2), 3.10 (brs, 4H, piperazine-CH_2), 3.41 (s, 2H, CH_2), 6.82 (d, $J = 8.43$ Hz, 2H, Ar-H), 7.01 (d, $J = 8.28$ Hz, 2H, Ar-H), 7.28 (td, J_1=9.04 Hz, J_2=2.57 Hz, H, Ar-H), 7.75 (q, J_1=4.77 Hz, J_2=8.90 Hz, H, Ar-H), 7.89 (dd, J_1=2.49 Hz, J_2=8.70 Hz, H, Ar-H), 12.06 (brs, H, NH). ^{13}CNMR (75 MHz, DMSO-d_6, ppm) δ 20.49 (CH_3), 49.14 (CH_2), 52.99 (piperazine-CH_2), 60.60 (piperazine-CH_2), 60.60 (CH_2), 108.47 and 108.82, 114.54 and 114.86,

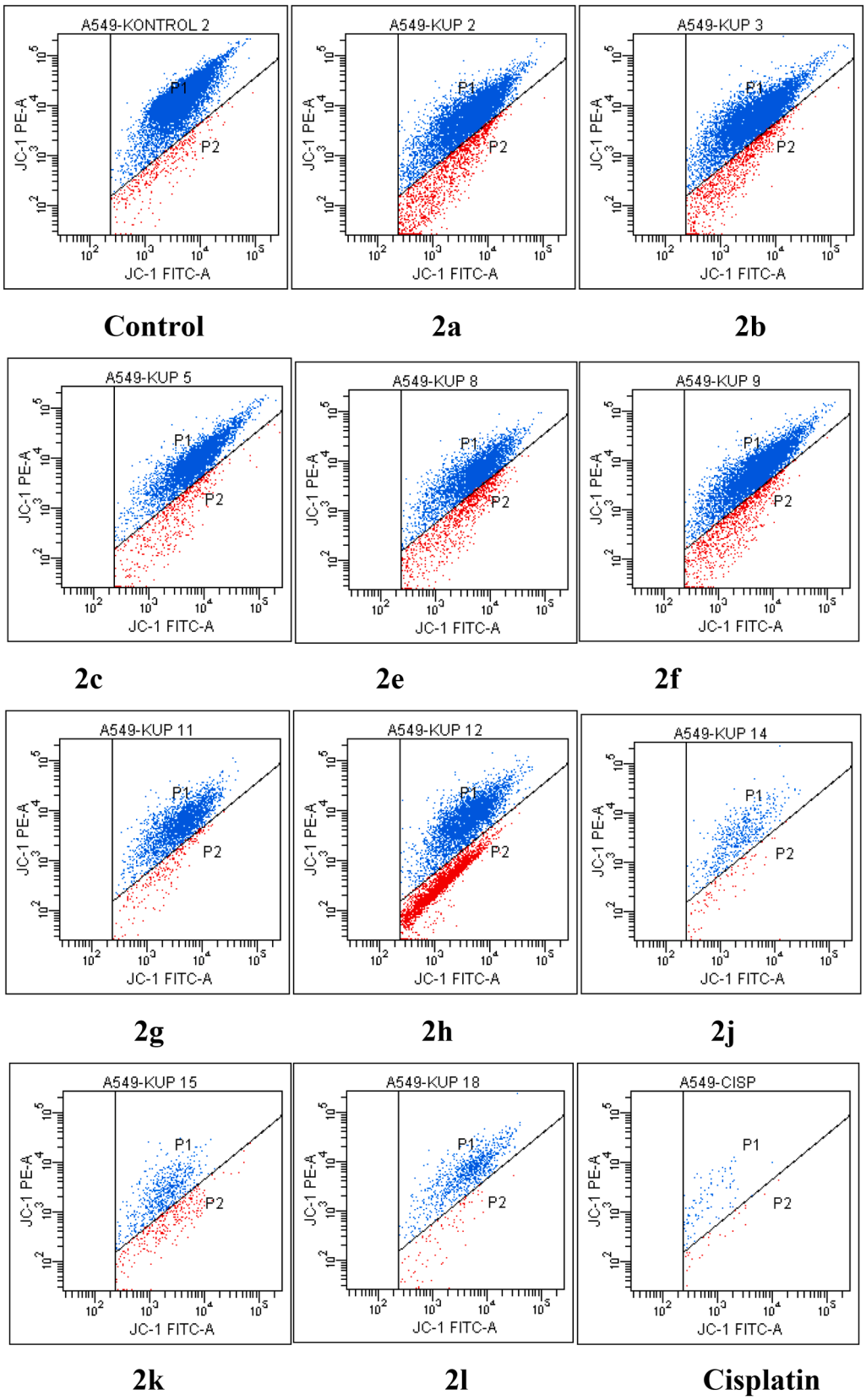

Fig. 3. Percentages of mitochondrial membrane polarization/depolarization of A549 cells after 24 h incubation with compounds **2a, 2b, 2c, 2e, 2f,** 2 g, 2 h, **2j, 2k, 2l** and cisplatin.

Table 5
Mitochondrial membrane polarization and depolarization percentages on A549 cell line.

Comp.	Depolarization%	Polarization%	Comp.	Depolarization%	Polarization%
2a	13.2	80.0	**2 g**	7.7	90.2
2b	9.7	85.9	**2h**	41.2	55.2
2c	9.7	88.1	**2i**	11.9	79.6
2e	19.7	76.7	**2j**	28.3	60.5
2f	11.2	85.5	**2l**	8.5	88.5
Control	3.4	95.3	**R.D.**	14.2	48.9

R.D.: Reference Drug (cisplatin).

Table 6
The effect on cell cycle of the selected compounds.

Compounds	% G0/G1 Phase	% S Phase	% G2/M Phase
Control	48.35	12.95	20.61
Compound 2b	59.74	6.93	19.14
Compound 2e	69.18	5.84	18.89
Compound 2 g	51.94	12.72	11.66
Compound 2h	48.15	11.95	12.63
Cisplatin	54.45	4.56	18.51

116.18, 122.03 and 122.15, 128.11, 129.81, 145.65, 149.39, 157.54, 157.97 and 158, 160.72, 169.94 (C = O). For $C_{20}H_{21}FN_4OS$ calculated: Elemental Analysis:%C 62.48;%H 5.51;%N 14.57; found:%C 62.47;%H 5.50;%N 14.58. HRMS (*m/z*): $[M + 1]^+$ calculated 385.1493; found 385.1488.

4.1.4. 2-(4-(4-Chlorophenyl) piperazin-1-yl)-N-(6-fluorobenzothiazol-2-yl)acetamide (2b)

Light brown solid, yield 72%, m. p. 160 °C, ^{1}HNMR (300 MHz, DMSO-d_6, ppm) δ 2.69 (brt, *J1*=4.59 Hz, 4H, piperazine-CH_2), 3.17 (brt, $J = 4.68$ Hz, 4H, piperazipiperazine-CH_2), 3.43 (s, 2H, CH_2), 9.94 (d, $J =$ 9.05 Hz, 2H, Ar-H), 7.22 (d, $J = 8.97$ Hz, 2H, Ar-H), 7.30 (dd, J_1=2.66

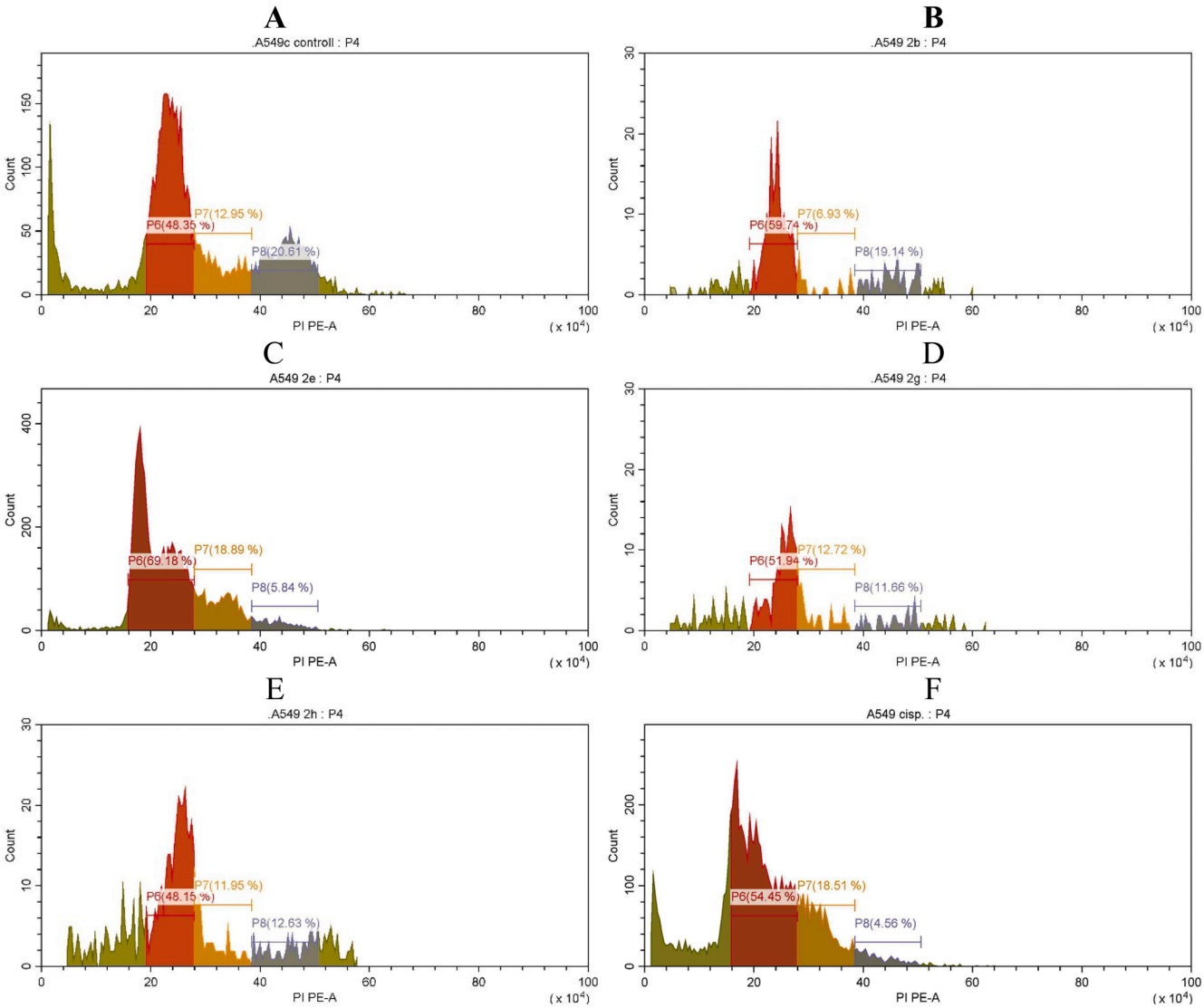

Fig. 4. Percentages of cell cycle involvement of A549 cells after 24 h incubation with no agent **(A), 2b (B), 2e (C), 2g (D), 2h (E)** and cisplatin **(F)**.

Table 7
MMP-9 inhibition percentages of the synthesized compounds (100 μg/mL).

Comp.	Inhibition%	Comp.	Inhibition%
2a	36.24 ± 2.28	**2 g**	10.24 ± 1.06
2b	30.66 ± 1.42	**2h**	16.46 ± 2.18
2c	38.72 ± 1.12	**2i**	8.52 ± 1.38
2d	—	**2j**	—
2e	46.36 ± 2.12	**2k**	26.0 ± 0.62
2f	48.56 ± 1.80	**NNGH (1.3 μM)**	91.59 ± 0.68

NNGH: *N*-Isobutyl-*N*-(4-methoxyphenylsulfonyl)glycyl hydroxamic acid, it was tested at 1.3 μM/mL concentration for determining inhibition% on MMP-9. **—**: No inhibition.

Hz, J_2=9.07 Hz, H, Ar-H), 7.75 (q, J_1=4.84 Hz, J_2=8.86 Hz, H, Ar-H), 7.89 (dd, J_1=2.65 Hz, J_2=8.74 Hz, H, Ar-H), 12.20 (brs, H, NH). ^{13}CNMR (75 MHz, DMSO-d_6, ppm) δ 48.43 (piperazine-CH_2), 52.75 (piperazine-CH_2), 60.45 (CH_2), 108.47 and 108.83, 114.55 and 114.87, 117.35, 122.04 and 122.16, 122.81, 129.06, 145.65, 150.23, 157.54, 157.95 and 157.98, 160.72, 169.85 (C = O). For $C_{19}H_{18}ClFN_4OS$ calculated: Elemental Analysis:%C 56.36;%H 4.48;%N 13.84; found:%C 56.35;%H 4.47;%N 13.83. HRMS (*m/z*): $[M+1]^+$ calculated 405.0947; found 405.0941.

4.1.5. N-(benzothiazol-2-yl)−2-(4-(p-tolyl) piperazin-1-yl)acetamide (2c)

Brown powder, yield 75%, m. p. 169 °C, ^{1}HNMR (300 MHz, DMSO-d_6, ppm) δ 2.18 (s, 3H, CH3), 2.67 (brs, 4H, piperazine-CH_2), 3.08 (brs, 4H, piperazine-CH_2), 3.41 (s, 2H, CH_2), 6.80 (d, J = 8.53 Hz, 2H, Ar-H), 7.00 (d, J = 8.40 Hz, 2H, Ar-H), 7.30 (t, J = 7.71 Hz, H, Ar-H), 7.43 (t, J = 7.71 Hz, H, Ar-H), 7.75 (d, J = 7.87 Hz, H, Ar-H), 7.97 (d, J = 7.87 Hz, H, Ar-H), 12.43 (brs, H, NH). ^{13}CNMR (75 MHz, DMSO-d_6, ppm) δ 20.50 (CH_3), 49.14 (piperazine-CH_2), 52.99 (piperazine-CH_2), 60.68 (CH_2), 116.17, 121.00, 122.16, 124.06, 126.59, 128.11, 129.81, 131.95, 148.93, 149.37, 157.98, 169.85 (C = O). For $C_{20}H_{22}N_4OS$ calculated: Elemental Analysis:%C 65.55;%H 6.05;%N 15.29; found:%C 65.54;%H 6.04;%N 15.28. HRMS (*m/z*): $[M+1]^+$ calculated 367.1587; found 367.1577.

4.1.6. N-(benzothiazol-2-yl)−2-(4-(4-chlorophenyl) piperazin-1-yl) acetamide (2d)

Off-white powder, yield 77%, m. p. 155 °C, ^{1}HNMR (300 MHz, DMSO-d_6, ppm) δ 2.68 (brs, 4H, piperazine-CH_2), 3.16 (brs, 4H, piperazine-CH_2), 3.42 (s, 2H, CH2), 6.91 (d, 2H, J = 9.26 Hz, 2H, Ar-H), 7.22 (d, J = 8.73 Hz, 2H, Ar-H), 7.30 (brt, J = 7.43 Hz, H, Ar-H), 7.43 (brt, J = 7.70 Hz, H, Ar-H), 7.75 (d, J = 7.92 Hz, H, Ar-H), 7.98 (d, J = 7.65 Hz, H, Ar-H), 12.40 (brs, H, NH). ^{13}CNMR (75 MHz, DMSO-d_6, ppm) δ 48.47 (piperazine-CH_2), 52.77 (piperazine-CH_2), 60.57 (CH_2), 117.33, 121.00, 122.18, 122.80, 124.05, 126.59, 129.06, 131.94, 148.93, 150.23, 157.97, 169.82 (C = O). For $C_{19}H_{19}ClN_4OS$ calculated: Elemental Analysis:%C 58.98;%H 5.80;%N 14.65; found:%C 58.99;%H 5.81;%N 14.66. HRMS (*m/z*): $[M+1]^+$ calculated 387.1041; found 387.1045.

4.1.7. N-(6-methoxybenzothiazol-2-yl)−2-(4-(p-tolyl) piperazin-1-yl) acetamide (2e)

Orangish powder, yield 70%, m. p. 162 °C, ^{1}HNMR (300 MHz, DMSO-d_6, ppm) δ 2.18 (s, 3H, CH_3), 2.68 (s, 4H, piperazine-CH_2), 3.09 (s, 4H, piperazine-CH_2), 3.39 (s, 2H, CH_2), 3.80 (s, 3H, O—CH_3), 6.79–6.86 (m, 2H, Ar-H), 6.98–7.05 (m, 3H, Ar-H), 7.56 (d, J = 2.50 Hz, H, Ar-H), 7.64 (d, J = 8.85 Hz, H, Ar-H), 11.24 (brs, H, NH). ^{13}CNMR (75 MHz, DMSO-d_6, ppm) δ 20.50 (CH_3), 49.15 (piperazine-CH_2), 53.01 (piperazine-CH_2), 56.07 (J = 2.42 Hz, O—CH_3), 60.53 (CH_2), 105.18, 115.38, 116.17, 116.60, 121.60, 128.09, 129.81, 129.95, 133.27, 143.04, 149.39, 155.91, 156.64, 169.53 (C = O). For $C_{21}H_{24}N_4O_2S$ calculated: Elemental Analysis:%C 63.61;%H 6.10;%N 14.13; found:%C 63.62;%H 6.11;%N 14.12. HRMS (*m/z*): $[M+1]^+$ calculated 397.1693; found 397.1681.

4.1.8. 2-(4-(4-Chlorophenyl) piperazin-1-yl)-N-(6-methoxybenzothiazol-2-yl)acetamide (2f)

Yellowish powder, yield 73%, m. p. 203 °C, ^{1}HNMR (300 MHz, DMSO-d_6, ppm) δ 2.68 (brt, J = 8.84 Hz, 4H, piperazine-CH_2), 3.16 (brt, J = 8.82 Hz, 4H, piperazine-CH_2), 3.94 (s, 2H, CH_2), 3.80 (s, 3H, O—CH_3), 6.92 (d, J = 9.07, 2H, Ar-H), 7.03 (dd, J_1=2.57 Hz, J_2=8.92 Hz, H, Ar-H), 7.21 (d, J = 8.99 Hz, 2H, Ar-H), 7.57 (d, J = 2.51 Hz, H, Ar-H), 7.64 (d, J = 8.83 Hz, H, Ar-H), 10.94 (brs, H, NH). ^{13}CNMR (75 MHz, DMSO-d_6, ppm) δ 48.48 (piperazine-CH_2), 52.78 (piperazine-CH_2), 56.01 (J = 2.28 Hz, O—CH_3), 60.54 (CH_2), 105.18, 115.39, 117.32, 121.60, 122.80, 129.05, 133.26, 143.02, 150.23, 155.91, 156.64, 169.50 (C = O). For $C_{20}H_{21}ClN_4O_2S$ calculated: Elemental Analysis:%C 57.62;%H 5.08;%N 13.44; found:%C 57.63;%H 5.09;%N 13.45. HRMS (*m/z*): $[M+1]^+$ calculated 417.1147; found 417.1146.

*4.1.9. **N-(6-methylbenzothiazol-2-yl)−2-(4-(p-tolyl) piperazin-1-yl) acetamide (2 g)***

Orangish powder, yield 76%, m. p. 163 °C, ^{1}HNMR (300 MHz, DMSO-d_6, ppm) δ 2.19 (s, 3H, phenyl-CH_3), 2.40 (s, 3H, CH_3), 2.68 (brt, J = 9.44 Hz, 4H, piperazine-CH_2), 3.09 (brt, J = 9.48 Hz, 4H, piperazine-CH_2), 3.40 (s, 2H, CH_2), 6.81 (d, J = 8.59 Hz, 2H, Ar-H), 7.01 (d, J = 8.47 Hz, 2H, Ar-H), 7.24 (dd, J_1=1.42 Hz, J_2=8.51 Hz, H, Ar-H), 7.63 (d, J = 8.21 Hz, H, Ar-H), 7.74 (brd, J = 0.69 Hz, H, Ar-H), 11.24 (brs, H, NH). ^{13}CNMR (75 MHz, DMSO-d_6, ppm) δ 20.50 (phenyl-CH_3), 21.44

Table 8
Some characteristics of the synthesized compounds.

	Physicochemical Properties							Druglikeness							Pharmacokinetics	
Compound	MW	Log P	Log S	TPSA	HBA	HBD	MV	DLMS	A	B	C	D	E	F	GI	BBB
2a	384.14	4.25	−4.08	48.47	5	1	337.61	0.77	+	+	+	+	+	0.55	High	Yes
2b	404.09	4.48	−4.58	48.47	5	1	334.59	0.85	+	+	+	+	+	0.55	High	Yes
2c	366.15	4.11	−3.68	48.47	5	1	332.68	0.77	+	+	+	+	+	0.55	High	Yes
2d	386.10	4.34	−4.18	48.47	5	1	329.66	1.22	+	+	+	+	+	0.55	High	Yes
2e	396.16	4.14	−3.91	57.70	6	1	358.23	0.69	+	+	+	+	+	0.55	High	No
2f	416.11	4.37	−4.41	57.70	6	1	355.20	1.12	+	+	+	+	+	0.55	High	No
2 g	380.17	4.53	−4.09	48.47	5	1	349.24	0.47	+	+	+	+	+	0.55	High	Yes
2h	400.11	4.76	−4.59	48.47	5	1	346.22	0.89	+	+	+	+	+	0.55	High	Yes
2i	410.18	4.52	−4.35	57.70	6	1	375.03	0.55	+	+	+	+	+	0.55	High	No
2j	430.12	4.75	−4.85	57.70	6	1	372.00	0.97	+	+	+	+	+	0.55	High	No
2k	411.14	4.04	−4.54	94.29	8	1	356.01	0.12	+	+	+	+	+	0.55	High	No
2l	431.08	4.27	−5.05	94.29	8	1	352.99	0.48	+	+	+	+	+	0.55	High	No

MW: Molecular weight, **Log P:** Octanol/water partition coefficient, **Log S:** Aqueous solubility [in Log(moles/L)], **TPSA:** Topological polar surface area, **DLMS:** Druglikeness model score, **HBA:** Number of hydrogen acceptors, **HBD:** Number of hydrogen donors, **MV:** Molecular volume (A^3), DLMS, and MW were calculated by molsoft.com/mprop/software. Log P, TPSA HBA, HBD and molecular volume was calculated by www.molinspiration.com/cgi-bin/properties. Druglikeness and pharmacokinetics profiles were determined by SwissADME web tool (http://www.swissadme.ch). **A:** Lipinski, **B:** Ghose, **C:** Veber, **D:** Egan, **E:** Muegge (+ means appropriate in rule, **-** means inappropriate in rule), **F:** Bioavailability Score; **GI:** Gastrointestinal absorption, **BBB:** Blood-Brain barrier permeant.

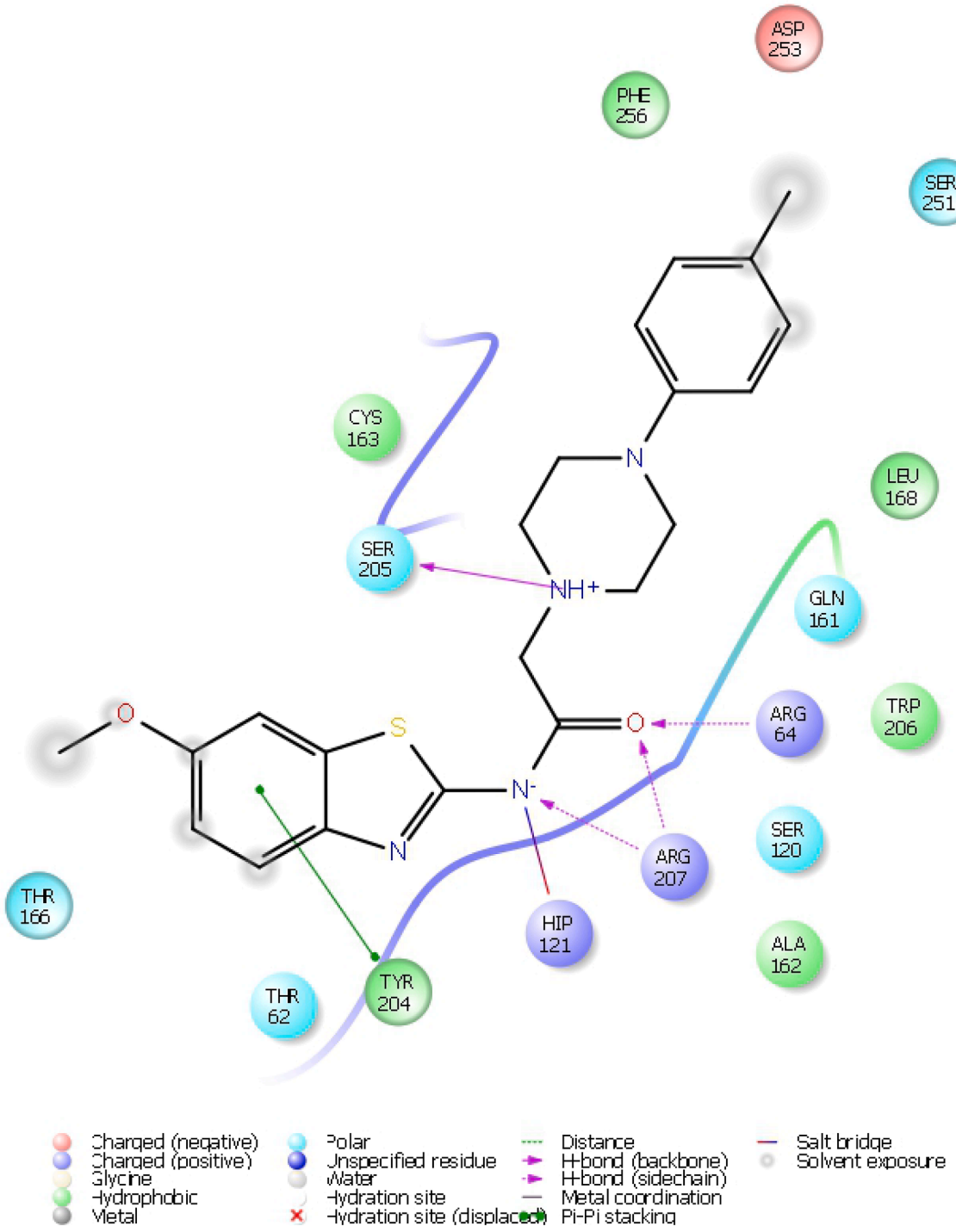

Fig. 5. 2D diagram of compound **2e** at caspase-3 active pocket (PDBID: 4EHA).

(CH_3), 49.15 (piperazine-CH_2), 53.00 (piperazine-CH_2), 60.67 (CH_2), 116.17, 120.63, 121.76, 127.91, 128.09, 129.81, 132.09, 133.50, 146.92, 149.39, 157.09, 169.68 (C = O). For $C_{21}H_{24}N_4OS$ calculated: Elemental Analysis:%C 66.29;%H 6.36;%N 14.72; found:%C 66.28;%H 6.35;%N 14.71. HRMS (*m/z*): $[M + 1]^+$ calculated 381.1744; found 381.1732.

4.1.10. 2-(4-(4-Chlorophenyl) piperazin-1-yl)-N-(6-methylbenzothiazol-2-yl)acetamide (2 h)

Off-white powder, yield 78%, m. p. 205 °C, ^{1}HNMR (300 MHz, DMSO-d_6, ppm) δ 2.40 (s, 3H, CH_3), 2.68 (brs, 4H, piperazine-CH_2), 3.16 (brs, 4H, piperazine-CH_2), 3.40 (s, 2H, CH_2), 6.92 (d, J = 8.64 Hz, 2H, Ar-H), 7.19–7.25 (m, 3H, Ar-H), 7.63 (d, J = 8.17 Hz, H, Ar-H), 7.74 (s, H, Ar-H), 11.71 (brs, H, NH). ^{13}CNMR (75 MHz, DMSO-d_6, ppm) δ 21.44 (CH_3), 48.48 (piperazine-CH_2), 52.77 (piperazine-CH_2), 60.56 (CH_2), 117.33, 120.64, 121.77, 122.79, 127.92, 129.06, 132.08, 133.51, 146.90, 150.24, 157.07, 169.65 (C = O). For $C_{20}H_{21}ClN_4OS$ calculated: Elemental Analysis:%C 59.92;%H 5.28;%N 13.97; found:%C 59.93;%H 5.29;%N 13.96. HRMS (*m/z*): $[M + 1]^+$ calculated 401.1197; found 401.1182.

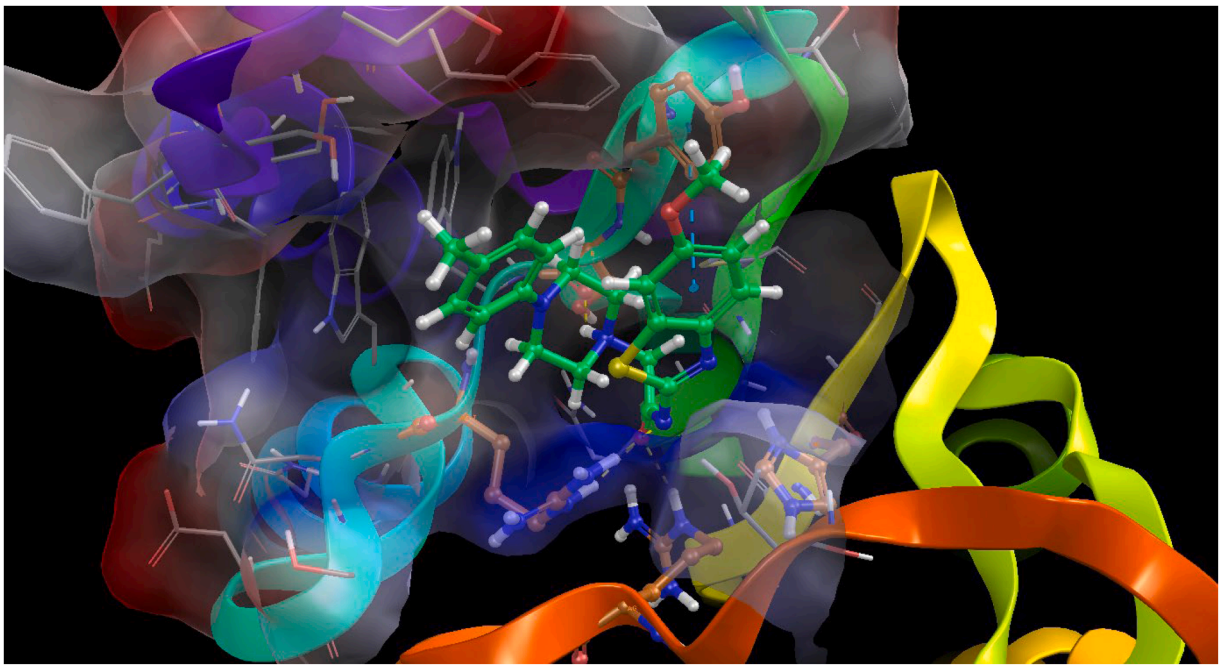

Fig. 6. Compound **2e** (Spring green carbon) at the pocket of caspase-3 (Orange carbon for interacted residues and gray carbon for other binding side residues. PDBID: 4EHA).

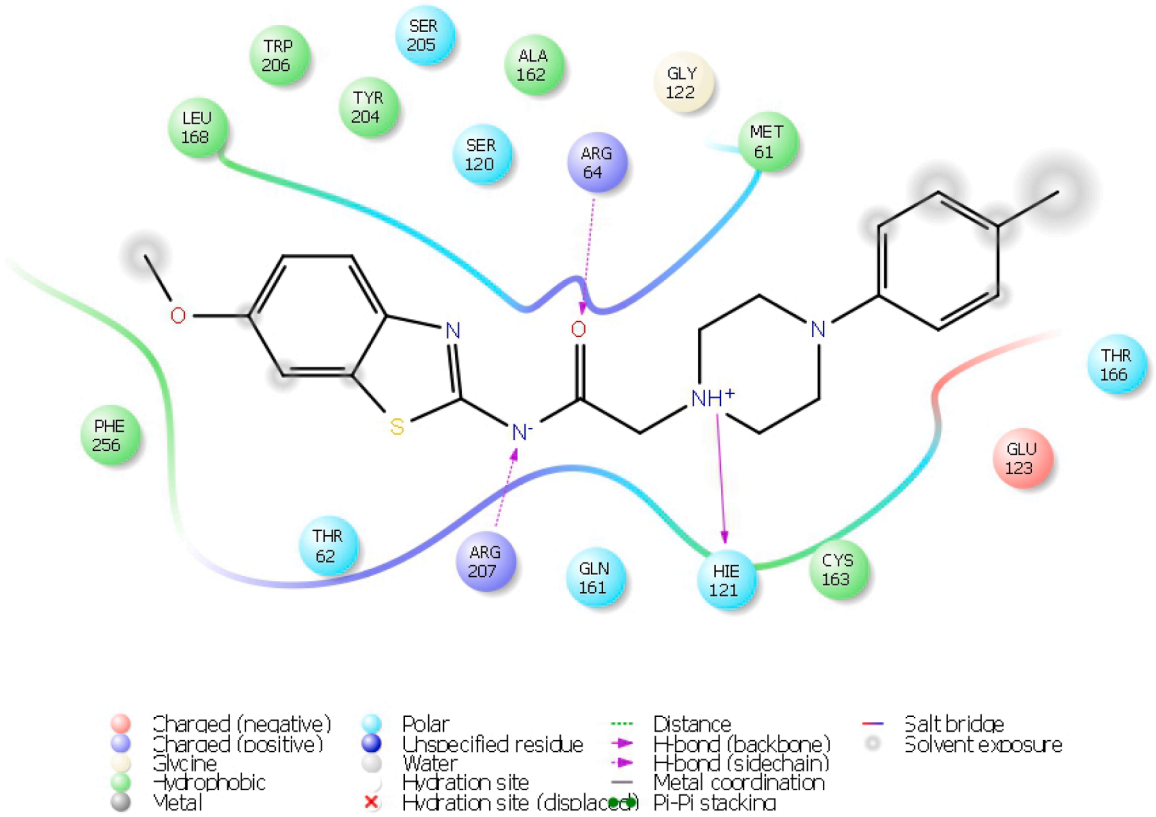

Fig. 7. 2D diagram of compound **2e** at caspase-3 active pocket (PDBID: 4QTX).

4.1.11. N-(6-ethoxybenzothiazol-2-yl)−2-(4-(p-tolyl) piperazin-1-yl) acetamide (2i)

Brown powder, yield 70%, m. p. 115 °C, ^{1}HNMR (300 MHz, DMSO-d_6, ppm) δ 1.34 (t, J = 6.86 Hz, 3H, ethoxy-CH_3), 2.18 (s, 3H, phenyl-CH_3), 2.67 (brs, 4H, piperazine-CH_2), 3.08 (brs, 4H, piperazine-CH_2), 3.38 (s, 2H, CH_2), 4.04 (q, J_1=6.87 Hz, J_2=13.52 Hz, 2H, ethoxy-CH_2), 6.80 (d, J = 8.46 Hz, 2H, Ar-H), 6–987.03 (m, 3H, Ar-H), 7.53 (s, H, Ar-H), 7.63 (d, J = 8.82 Hz, H, Ar-H), 11.96 (brs, H, NH). ^{13}CNMR (75 MHz, DMSO-d_6, ppm) δ 15.15 (ethoxy-CH_3), 20.49 (phenyl-CH_3), 49.15 (piperazine-CH_2), 53.01 (piperazine-CH_2), 60.66 (CH_2), 64.05 (ethoxy-

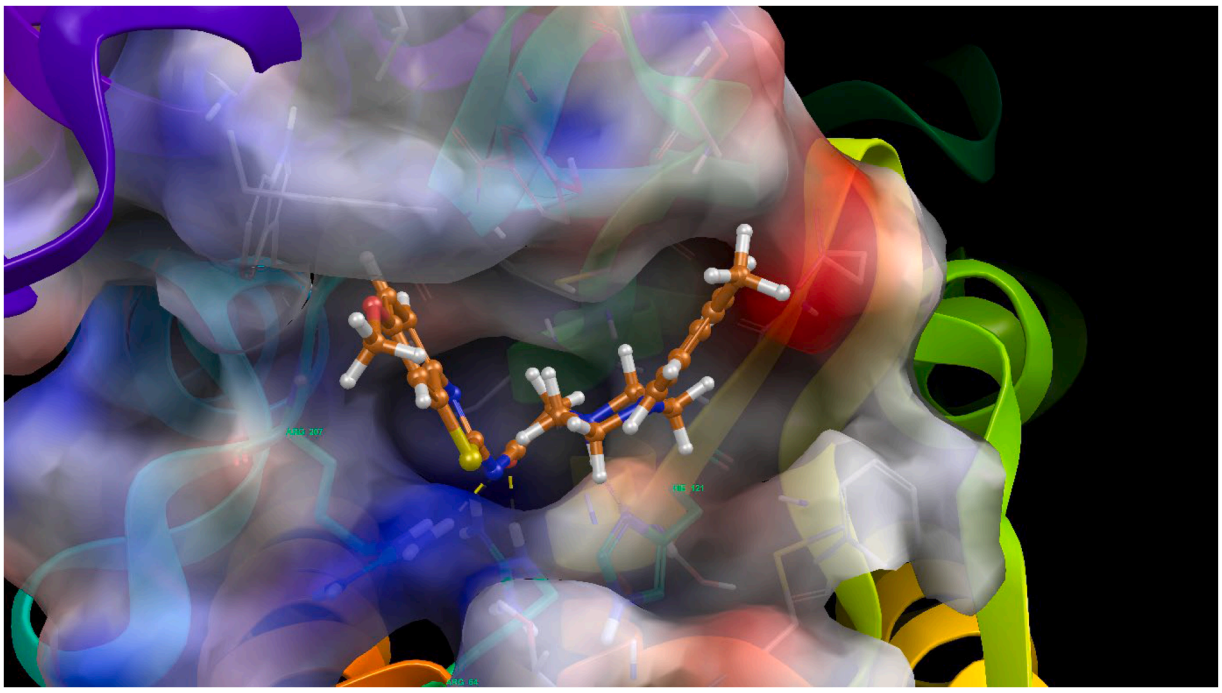

Fig. 8. Compound **2e** (Orange carbon) at the pocket of caspase-3 (Spring green carbon for interacted residues and gray carbon for other binding side residues. PDBID: 4QTX).

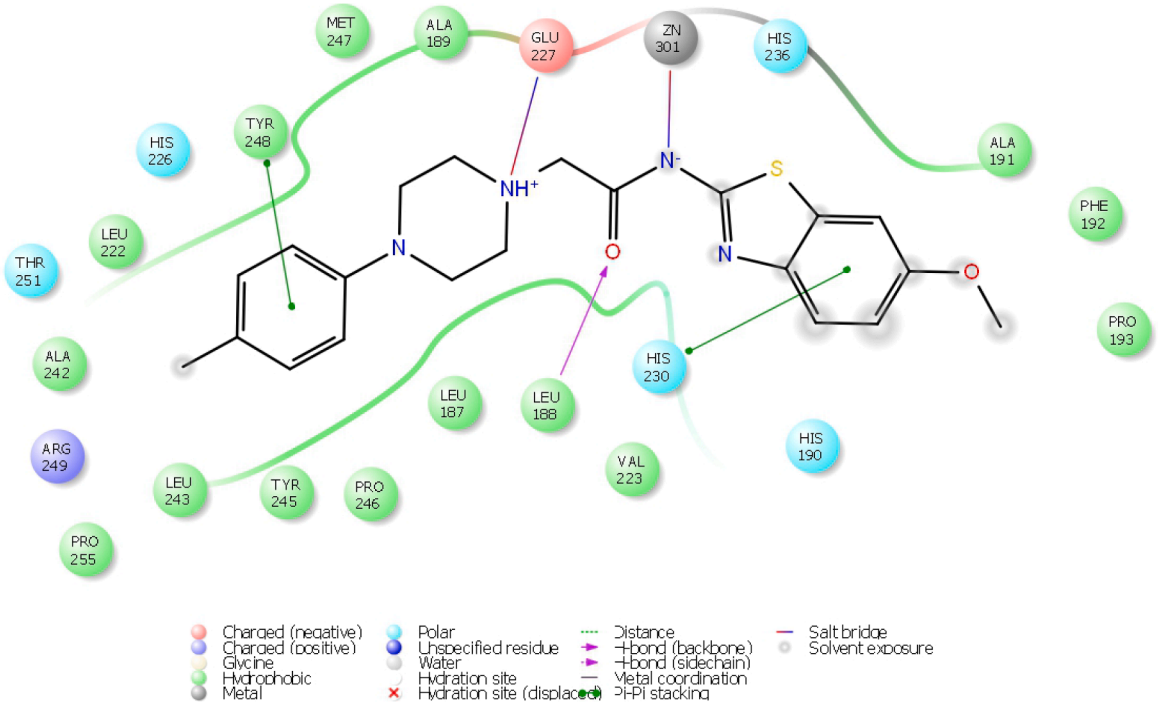

Fig. 9. 2D diagram of compound **2e** at active pocket of MMP-9 (PDBID: 5I12).

CH_2), 105.79, 115.72, 116.16, 121.59, 128.09, 129.80, 133.27, 142.97, 149.38, 155.89, 169.50 (C = O). For $C_{22}H_{26}N_4O_2S$ calculated: Elemental Analysis:%C 64.37;%H 6.38;%N 13.65; found:%C 64.38;%H 6.39;%N 13.66. HRMS (*m/z*): $[M + 1]^+$ calculated 411.1849; found 411.1841.

4.1.12. 2-(4-(4-Chlorophenyl) piperazin-1-yl)-N-(6-ethoxybenzothiazol-2-yl)acetamide (2j)

Brown powder, yield 75%, m. p. 160 °C, ^{1}HNMR (300 MHz, DMSO-d_6, ppm) δ 1.33 (t, J = 6.79 Hz, 3H, ethoxy-CH_3), 2.67 (brs, 4H, piperazine-CH_2), 3.14 (brs, 4H, piperazine-CH_2), 3.40 (s, 2H, CH_2), 4.04 (q, J_1=6.87 Hz, J_2=13.74 Hz, 2H, ethoxy-CH_2), 6.89 (d, J = 8.84 Hz, 2H, Ar-H), 7.01 (dd, J_1=2.18 Hz, J_2=8.74 Hz, H, Ar-H), 7.20 (d, J = 8.83 Hz, 2H, Ar-H), 7.53 (d, J = 2.11 Hz, H, Ar-H), 7.63 (d, J = 8.83 Hz, H, Ar-H), 11.97 (brs, H, NH). ^{13}CNMR (75 MHz, DMSO-d_6, ppm) δ 15.15 (ethoxy-CH_3), 48.46 (piperazine-CH_2), 52.78 (piperazine-CH_2), 60.54 (CH_2), 64.05 (ethoxy-CH_2), 105.79, 115.72, 117.30, 121.59, 122.82, 129.04,

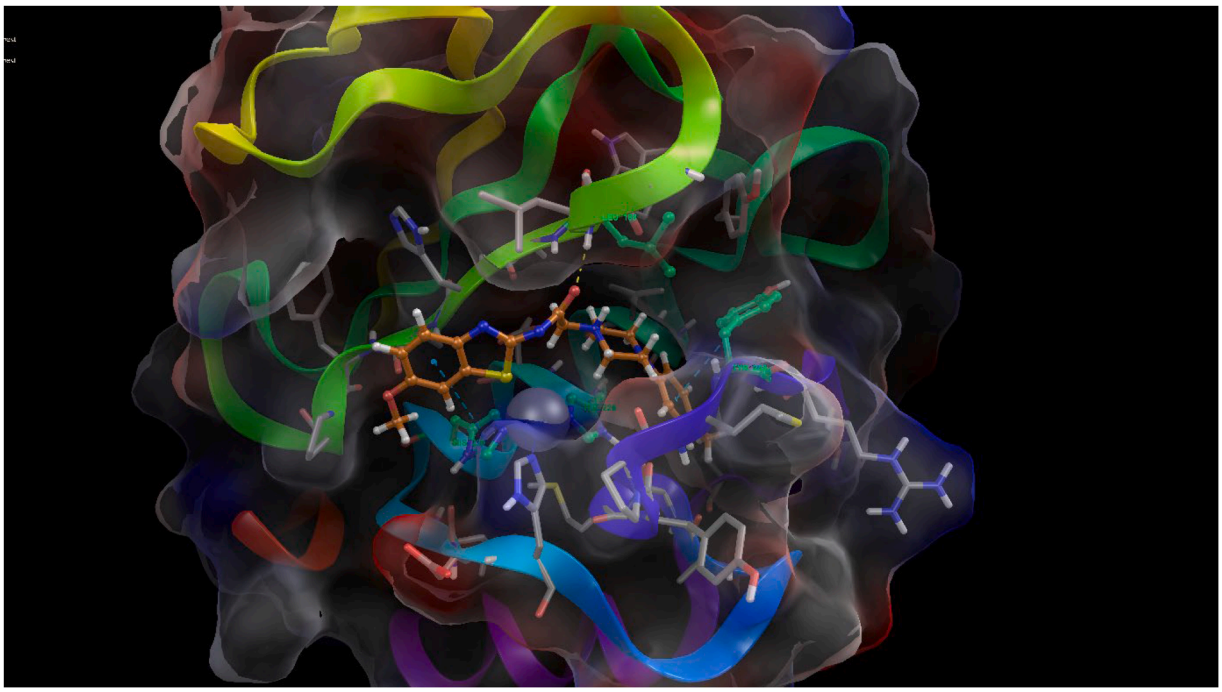

Fig. 10. Compound **2e** (Orange carbon) at the pocket of MMP-9 (Spring green carbon for interacted residues and gray carbon for other binding side residues. PDBID: 5I12).

133.26, 142.95, 150.21, 155.87, 169.45 (C = O). For $C_{21}H_{23}ClN_4O_2S$ calculated: Elemental Analysis:%C 58.53;%H 5.38;%N 13.00; found:%C 58.52;%H 5.39;%N 13.01. HRMS (*m/z*): $[M + 1]^+$ calculated 431.1303; found 431.1294. MS $[M + 1]$ +: *m/z* 431.1294.

4.1.13. N-(6-nitrobenzothiazol-2-yl)−2-(4-(p-tolyl) piperazin-1-yl) acetamide (2k)

Yellow solid, yield 81%, m. p. 229 °C, ^{1}HNMR (300 MHz, DMSO-d_6, ppm) δ 2.19 (s, 3H, CH_3), 2.70 (brt, 4.82 Hz, 4H, piperazine-CH_2), 3.12 (brt, J = 4.75 Hz, 4H, piperazine-CH_2), 3.47 (s, 2H, CH_2), 6.84 (d, J = 8.47 Hz, 2H, Ar-H), 7.02 (d, J = 8.47 Hz, 2H, Ar-H), 7.90 (d, J = 9.06 Hz, H, Ar-H), 8.28 (dd, J_1=2.43 Hz, J_2=8.90 Hz, H, Ar-H), 9.06 (d, J = 2.37 Hz, H, Ar-H), 12.60 (brs, H, NH). ^{13}CNMR (75 MHz, DMSO-d_6, ppm) δ 20.51 (CH_3), 49.11 (piperazine-CH_2), 52.94 (piperazine-CH_2), 60.59 (CH_2), 116.20, 119.53, 121.05, 122.25, 128.13, 129.82, 132.67, 143.47, 149.38, 153.88, 163.62, 170.62 (C = O). For $C_{20}H_{21}N_5O_3S$ calculated: Elemental Analysis:%C 58.38;%H 5.14;%N 17.02; found:%C 58.37;%H 5.15;%N 17.01. HRMS (*m/z*): $[M + 1]^+$ calculated 412.1438; found 412.1419.

4.1.14. 2-(4-(4-Chlorophenyl) piperazin-1-yl)-N-(6-nitrobenzothiazol-2-yl)acetamide (2l)

Light brown solid, yield 80%, m. p. 183 °C, ^{1}HNMR (300 MHz, DMSO-d_6, ppm) δ 2.71 (brs, 4H, piperazine-CH_2), 3.17 (brs, 4H, piperazine-CH_2), 3.48 (s, 2H, CH_2), 6.92 (d, J = 8.71 Hz, 2H, Ar-H), 7.21 (d, J = 8.59 Hz, 2H, Ar-H), 7.86 (d, J = 8.87 Hz, H, Ar-H), 8.23–8.27 (m, H, Ar-H), 9.01 (s, H, Ar-H), 12.55 (brs, H, NH). ^{13}CNMR (75 MHz, DMSO-d_6, ppm) δ 48.42 (piperazine-CH_2), 52.71 (piperazine-CH_2), 60.46 (CH_2), 117.32, 119.43, 121.00, 122.17, 122.82, 129.04, 132.64, 143.43, 150.20, 153.83, 163.53, 170.52 (C = O). For $C_{19}H_{18}ClN_5O_3S$ calculated: Elemental Analysis:%C 52.84;%H 4.20;%N 16.22; found%C 52.85;%H 4.21;%N 16.23. HRMS (*m/z*): $[M + 1]^+$ calculated 432.0892; found 432.0872.

4.2. Biochemistry

4.2.1. Model cell line

The human lung adenocarcinoma (A549), rat glioma (C6) and mouse embryonic fibroblast (NIH/3T3) cells were maintained in 75 cm^2 sterile plastic tissue culture flasks in 90% RPMI (Sigma, Deisenhofen, Germany) medium supplemented with%10 (v/v) FBS (Gibco, Paisley, UK) and penicillin/streptomycin (Gibco, Paisley, UK) (100 units/mL) as adherent monolayers. These cells were grown at 37 °C in a humidified atmosphere containing%5 CO_2 in air. These methods were applied previously [51,58,72]

4.2.2. Cell viability analysis

MTT (3-(4,5-dimethylthiazol-2-yl)−2,5-diphenyltetrazolium bromide) approach was used to measure the cytotoxicity of the tested compounds against NIH/3T3, C6 and A549 cell lines according to the reported data [73,74]. The A549, C6, and NIH/3T3 cells were cultured at a density of 5 × 10^3 cells per well in flat bottomed 96-well plates. All of the synthesized compounds with various concentrations (50-1000 μM) and cisplatin as control drug was dissolved in DMSO. The next steps were run as same in our previous works [58,62].

4.2.3. The determination of early/late apoptosis by flow cytometry

After the A549, C6 and NIH/3T3 cells were incubated with the most potent antiproliferative agents in this series at their IC_{50} concentrations, phosphatidylserine externalization, which indicates early apoptosis, was measured by the FITC Annexin V apoptosis detection kit (BD Pharmingen, San Jose, CA, USA) on a BD FACSAria flow cytometer for 24 h. The A549 and NIH/3T3 cells were harvested and washed twice with ice-cold PBS and resuspended in 100 μL of binding buffer. A volume of 5 μL (5 μg/mL) of Annexin V-FITC and PI were added to the cells and incubated for 15 min in the dark at room temperature (20–25 °C). Then, 400 μL of binding buffer was added to the mixture samples and analyzed on a BD FACSAria flow cytometer using FACSDiva version 6.1.1 software (BD Biosciences, San Jose, CA, USA). Similar procedures [59,75,76] were used to investigated.

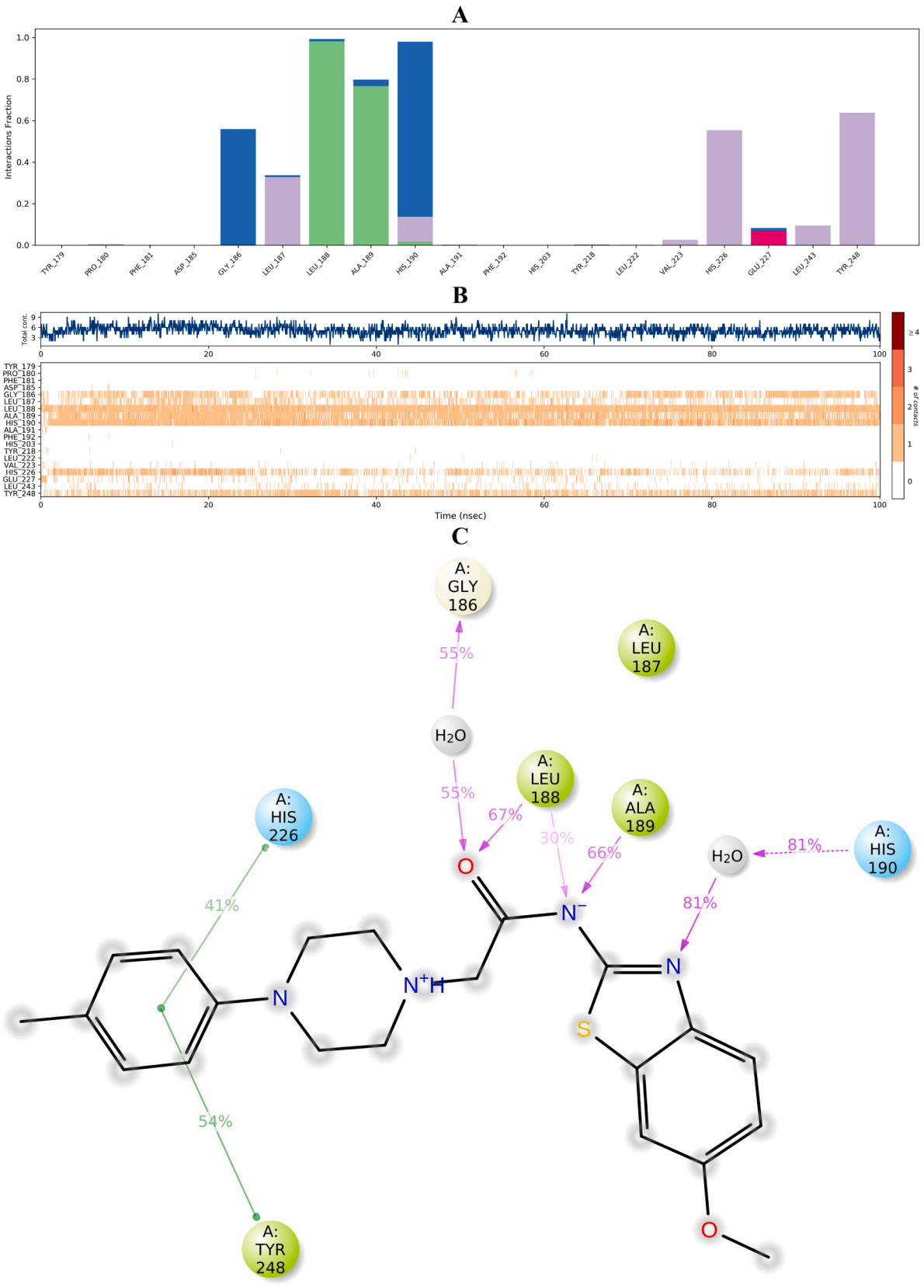

Fig. 11. MDS interaction plots of the 2e-MMP-9 system. **A)** Interaction type- Interaction fractions-residue index, **B)** Total interaction number-residue-time plot, **C)** 2D plot of contact strength (cut off=0.3).

4.2.4. Cell cycle analysis

After A549 cells were incubated with compounds for 24 h cell cycle analyses measurement protocol was applied according to the manufacturer's instructions (BD, Biosciences). This method was applied recently in our previous study [58].

4.2.5. Spectrofluorometric analysis of caspase-3 activation

Caspase-3 activation was analyzed by Spectrofluorometric Caspase-3 Assay kit (BD Pharmingen, Franklin Lakes, NJ). This experiment was performed according to Yurttaş et al. [77]..

4.2.6. Mitochondrial membrane depolarization determination assay

Staining of cells with JC-1 was realized according to the manufacturer's recommendations of BD, Pharmingen Flow cytometry kit. After determining the most active compounds by MTT method, the mitochondrial membrane integrity of the compounds on A549 cells was established based on their IC_{50} concentrations. Cisplatin was used as a positive control and the results were compared with this positive control [78]. This experiment was performed according to our previous work [62].

4.2.7. MMP-9 inhibition

MMP-9, colorimetric kits were purchased from EnzoLife Sciences Inc. (Farmingdale, New York, NY, USA). The MMP Colorimetric Drug Discovery Kits are a complete assay system designed to screen MMP inhibitors using a thiopeptide as a chromogenic substrate (Ac-PLG-[2-mercapto-4-methyl-pentanoyl]-LG-OC_2H_5). The same method was utilized in our previous work [50,62]. Similarly, NNGH was used as a control inhibitor. Data was expressed as Mean±SD. The inhibitor% remaining activity of MMPs was calculated using the following equation:

$$\text{Inhibitor\%activityremaining} = (\text{V inhibitor} / \text{Vcontrol}) \times 100.$$

The inhibition (percent) of MMPs was calculated using the following equation:

$$\text{I}(\%) = 100 - \text{Inhibitor\%activityremaining}$$

4.2.8. ADME parameters

Estimating some parameters such as drug-likeness profile, cheap, and easy synthesis in a short time, become indispensable in medicinal chemistry since these gain us some advantages [79-81].

Predictions of ADME properties of the obtained compounds **2a-2l** were calculated by the online Molinspiration property program [82], the Molsoft software [83] and SwissADME web-based tool [84]. The ligands were generated in smiles format and uploaded to these websites in this form.

4.3. In silico studies

4.3.1. Molecular docking studies

The primary aim of these molecular docking studies was to determine the binding mode between active ligand and protein structures due to *in vitro* results, thus, the molecular docking studies were run only for **2e**.

The crystal structures of the enzymes were retrieved from the Protein Data Bank server (PDB codes: 4EHA and 4QTX for caspase-3, 5I12 for MMP-9). Since the wild-type and mutation form of caspase-3 enzyme [85,86] are frequently encountered in cancer cells, both crystals were used. We also explain it in the procedure of molecular docking. The processes of protein preparation, ligand preparation, grid generation, docking and visualization studies were performed on Schrodinger's Maestro molecular modeling package [87,88] as in previous studies [51,54,89,90].

The water molecules were extracted from the crystal structures. Ligands were set to the physiological pH (pH 7.4 ± 1.0) at the protonation step. In molecular docking simulations, Glide/XP docking protocols were used for understanding the binding mode of compound **2e** with the active site of target proteins, then they were analyzed.

4.3.2. Molecular dynamics simulation study

The MDS technique is more realistic than the molecular docking study since the binding mode between ligand and protein, and the system stability can be analyzed as 4-dimensional [91-94]. Additionally, we can observe the environmental changes and their effects on binding mode during the simulation [95]. The methodology was applied as same as our previous studies [53,66,89,92,96]. Briefly, the best docking pose was carried out. The MDS was performed on Desmond application [97] using the standard force field (OPLS3e) of Schrodinger Suite with a transferable intermolecular potential with 3 points (TIP3P) water model followed by energy minimization of the complex. The neutralization of the system was achieved using Na^+ and Cl^- ions and 150 mM NaCl was added into dynamics condition. The molecular dynamics simulation was performed following the completion of the system setup. The radius of gyration (Rg), root mean square fluctuation (RMSF), and root mean square deviation (RMSD) values were calculated by Desmond application.

Ethics approval and consent to participate

Not applicable.

Human and animal rights

Not applicable.

Consent for publication

Not applicable.

CRediT authorship contribution statement

Asaf Evrim EVREN: Writing – review & editing, Writing – original draft, Software, Methodology, Investigation, Formal analysis, Data curation, Conceptualization. **Büşra EKSELLİ:** Writing – original draft, Investigation, Formal analysis. **Leyla YURTTAŞ:** Writing – review & editing, Writing – original draft, Supervision, Resources, Project administration, Methodology, Formal analysis, Conceptualization. **Halide Edip TEMEL:** Writing – original draft, Software, Investigation, Formal analysis, Data curation. **Gülşen AKALİN ÇİFTÇİ:** Writing – original draft, Validation, Resources, Project administration, Methodology, Investigation, Funding acquisition, Formal analysis.

Declaration of competing interest

The authors declare that they have no known competing financial interests or personal relationships that could have appeared to influence the work reported in this paper.

Data availability

No data was used for the research described in the article.

Acknowledgments

This study was supported by the Anadolu University Scientific Research Project, Eskisehir, Turkey (Project no: 1705S174).

Supplementary materials

Supplementary material associated with this article can be found, in

the online version, at doi:10.1016/j.molstruc.2024.139732.

References

[1] T.N. Seyfried, L.C. Huysentruyt, On the origin of cancer metastasis, Crit. Rev. Oncog. 18 (2013) 43–73, https://doi.org/10.1615/critrevoncog.v18.i1-2.40.

[2] K.F. Grossmann, K. Margolin, Long-term survival as a treatment benchmark in melanoma: latest results and clinical implications, Ther. Adv. Med. Oncol. 7 (2015) 181–191, https://doi.org/10.1177/1758834015572284.

[3] S. Korfee, T. Gauler, R. Hepp, C. Pottgen, W. Eberhardt, New targeted treatments in lung cancer–overview of clinical trials, Lung Cancer 45 (Suppl 2) (2004) S199–S208, https://doi.org/10.1016/j.lungcan.2004.07.974.

[4] C.S. Dela Cruz, L.T. Tanoue, R.A. Matthay, Lung cancer: epidemiology, etiology, and prevention, Clin. Chest Med. 32 (2011) 605–644, https://doi.org/10.1016/j.ccm.2011.09.001.

[5] C. Holohan, S. Van Schaeybroeck, D.B. Longley, P.G. Johnston, Cancer drug resistance: an evolving paradigm, Nat. Rev. Cancer 13 (2013) 714–726, https://doi.org/10.1038/nrc3599.

[6] J. Foo, F. Michor, Evolution of acquired resistance to anti-cancer therapy, J. Theor. Biol. 355 (2014) 10–20, https://doi.org/10.1016/j.jtbi.2014.02.025.

[7] D.K.W. Ocansey, F. Qian, P. Cai, S. Ocansey, S. Amoah, Y. Qian, F. Mao, Current evidence and therapeutic implication of PANoptosis in cancer, Theranostics 14 (2024) 640–661, https://doi.org/10.7150/thno.91814.

[8] V. Birukova, A. Scherbakov, A. Ilina, D. Salnikova, O. Andreeva, Y. Dzichenka, I. Zavarzin, Y. Volkova, Discovery of highly potent proapoptotic antiestrogens in a series of androst-5,16-dienes D-modified with imidazole-annulated pendants, J. Steroid. Biochem. Mol. Biol. 231 (2023) 106309, https://doi.org/10.1016/j.jsbmb.2023.106309.

[9] M.H. Mahnashi, F.F. El-Senduny, M.A. Alshahrani, M.A. Abou-Salim, Design, Synthesis, and Biological Evaluation of a Novel VEGFR-2 Inhibitor Based on a 1,2,5-Oxadiazole-2-Oxide Scaffold with MAPK Signaling Pathway Inhibition, Pharmaceuticals. (Basel) 15 (2022) 246, https://doi.org/10.3390/ph15020246.

[10] A. Siddiqui-Jain, J. Bliesath, D. Macalino, M. Omori, N. Huser, N. Streiner, C.B. Ho, K. Anderes, C. Proffitt, S.E. O'Brien, J.K. Lim, D.D. Von Hoff, D.M. Ryckman, W. G. Rice, D. Drygin, CK2 inhibitor CX-4945 suppresses DNA repair response triggered by DNA-targeted anticancer drugs and augments efficacy: mechanistic rationale for drug combination therapy, Mol. Cancer Ther. 11 (2012) 994–1005, https://doi.org/10.1158/1535-7163.MCT-11-0613.

[11] L. Liu, M. Hussain, J. Luo, A. Duan, C. Chen, Z. Tu, J. Zhang, Synthesis and biological evaluation of novel dasatinib analogues as potent DDR1 and DDR2 kinase inhibitors, Chem. Biol. Drug Des. 89 (2017) 420–427, https://doi.org/10.1111/cbdd.12863.

[12] A. Morabito, R. Costanzo, A.M. Rachiglio, R. Pasquale, C. Sandomenico, R. Franco, A. Montanino, E. De Lutio, G. Rocco, N. Normanno, Activity of gefitinib in a non-small-cell lung cancer patient with both activating and resistance EGFR mutations, J. Thorac. Oncol. 8 (2013) e59–e60, https://doi.org/10.1097/JTO.0b013e318286cc26.

[13] J. Wu, L. Yu, F. Yang, J. Li, P. Wang, W. Zhou, L. Qin, Y. Li, J. Luo, Z. Yi, M. Liu, Y. Chen, Optimization of 2-(3-(arylalkyl amino carbonyl) phenyl)-3-(2-methoxyphenyl)-4-thiazolidinone derivatives as potent antitumor growth and metastasis agents, Eur. J. Med. Chem. 80 (2014) 340–351, https://doi.org/10.1016/j.ejmech.2014.04.068.

[14] A.T. Shaw, J.A. Engelman, ALK in lung cancer: past, present, and future, J. Clin. Oncol. 31 (2013) 1105–1111, https://doi.org/10.1200/JCO.2012.44.5353.

[15] A. Sato, A. Shimotsuma, T. Miyoshi, Y. Takahashi, N. Funayama, Y. Ogino, A. Hiramoto, Y. Wataya, H.S. Kim, Extracellular Leakage Protein Patterns in Two Types of Cancer Cell Death: necrosis and Apoptosis, ACS. Omega 8 (2023) 25059–25065, https://doi.org/10.1021/acsomega.3c01691.

[16] M. Mancini, D.W. Nicholson, S. Roy, N.A. Thornberry, E.P. Peterson, L.A. Casciola-Rosen, A. Rosen, The caspase-3 precursor has a cytosolic and mitochondrial distribution: implications for apoptotic signaling, J. Cell Biol. 140 (1998) 1485–1495, https://doi.org/10.1083/jcb.140.6.1485.

[17] V. Juric, C. O'Sullivan, E. Stefanutti, M. Kovalenko, A. Greenstein, V. Barry-Hamilton, I. Mikaelian, J. Degenhardt, P. Yue, V. Smith, A. Mikels-Vigdal, MMP-9 inhibition promotes anti-tumor immunity through disruption of biochemical and physical barriers to T-cell trafficking to tumors, PLoS ONE 13 (2018) e0207255, https://doi.org/10.1371/journal.pone.0207255.

[18] M. Durcik, A. Nyerges, Z. Skok, D.G. Skledar, J. Trontelj, N. Zidar, J. Ilas, A. Zega, C.D. Cruz, P. Tammela, M. Welin, Y.R. Kimbung, D. Focht, O. Benek, T. Revesz, G. Draskovits, P.E. Szili, L. Daruka, C. Pal, D. Kikelj, L.P. Masic, T. Tomasic, New dual ATP-competitive inhibitors of bacterial DNA gyrase and topoisomerase IV active against ESKAPE pathogens, Eur. J. Med. Chem. 213 (2021) 113200, https://doi.org/10.1016/j.ejmech.2021.113200.

[19] Z. Skok, M. Barancokova, O. Benek, C.D. Cruz, P. Tammela, T. Tomasic, N. Zidar, L. P. Masic, A. Zega, C.E.M. Stevenson, J.E.A. Mundy, D.M. Lawson, A. Maxwell, D. Kikelj, J. Ilas, Exploring the Chemical Space of Benzothiazole-Based DNA Gyrase B Inhibitors, ACS. Med. Chem. Lett. 11 (2020) 2433–2440, https://doi.org/10.1021/acsmedchemlett.0c00416.

[20] D.A. Sheik, L. Brooks, K. Frantzen, S. Dewhurst, J. Yang, Inhibition of the enhancement of infection of human immunodeficiency virus by semen-derived enhancer of virus infection using amyloid-targeting polymeric nanoparticles, ACS Nano 9 (2015) 1829–1836, https://doi.org/10.1021/nn5067254.

[21] S. Sarkar, A.A. Siddiqui, S.J. Saha, R. De, S. Mazumder, C. Banerjee, M.S. Iqbal, S. Nag, S. Adhikari, U. Bandyopadhyay, Antimalarial Activity of Small-Molecule Benzothiazole Hydrazones, Antimicrob. Agents Chemother 60 (2016) 4217–4228, https://doi.org/10.1128/AAC.01575-15.

[22] Ü.D. Özkay, Ö.D. Can, Y. Özkay, Y. Öztürk, Effect of benzothiazole/piperazine derivatives on intracerebroventricular streptozotocin-induced cognitive deficits, Pharmacological Reports 64 (2012) 834–847, https://doi.org/10.1016/s1734-1140(12)70878-2.

[23] P. Zhang, M.F. Zou, A.L. Rodriguez, P.J. Conn, A.H. Newman, Structure-activity relationships in a novel series of 7-substituted-aryl quinolines and 5-substituted-aryl benzothiazoles at the metabotropic glutamate receptor subtype 5, Bioorg. Med. Chem. 18 (2010) 3026–3035, https://doi.org/10.1016/j.bmc.2010.03.053.

[24] M. Schubler, B. Sadek, T. Kottke, L. Weizel, H. Stark, Synthesis, Molecular Properties Estimations, and Dual Dopamine D2 and D3 Receptor Activities of Benzothiazole-Based Ligands, Front. Chem. 5 (2017) 64, https://doi.org/10.3389/fchem.2017.00064.

[25] S.H. Ferreira, B.B. Lorenzetti, M. Devissaguet, D. Lesieur, Y. Tsouderos, S14080, a peripheral analgesic acting by release of an endogenous circulating opioid-like substance, Br. J. Pharmacol. 114 (1995) 303–308, https://doi.org/10.1111/j.1476-5381.1995.tb13227.x.

[26] A. Francisco Nogueira, E. Carvalho Azevedo, V. Francisco Ferreira, A. Jersia Araujo, E. Alves dos Santos, C. Pessoa, L. Veras Costa-Lotufo, R. Carvalho Montenegro, M. Odorico de Moraes, T. Rocha Alves Vasconcelos, Synthesis and Antitumor Evaluation of (E)-2-Benzothiazole Hydrazones, Lett. Drug Des. Discov. 7 (2010) 551–555, https://doi.org/10.2174/157018010792062740.

[27] M.L. Zhu, C.Y. Wang, C.M. Xu, W.P. Bi, Z.H. XY, Evaluation of 6-chloro-N-[3,4-disubstituted-1,3-thiazol-2(3H)-ylidene]-1,3-benzothiazol-2-amine Using Drug Design Concept for Their Targeted Activity Against Colon Cancer Cell Lines HCT-116, HCT15, and HT29, Med. Sci. Monit. 23 (2017) 1146–1155, https://doi.org/10.12659/msm.899646.

[28] A. Irfan, F. Batool, S.A. Zahra Naqvi, A. Islam, S.M. Osman, A. Nocentini, S. A. Alissa, C.T. Supuran, Benzothiazole derivatives as anticancer agents, J Enzyme Inhib Med Ch 35 (2020) 265–279, https://doi.org/10.1080/14756366.2019.1698036.

[29] K. Haider, N. Shrivastava, A. Pathak, R. Prasad Dewangan, S. Yahya, M. Shahar Yar, Recent advances and SAR study of 2-substituted benzothiazole scaffold based potent chemotherapeutic agents, Results. Chem. 4 (2022) 100258, https://doi.org/10.1016/j.rechem.2021.100258.

[30] M. Charehsaz, E.E. Gürdal, S. Helvacıoğlu, M. Yarım, Piperazin halkası taşıyan benzotiyazol türevlerinin toksikolojik değerlendirilmesi, Marmara Pharm. J. 21 (2017) 243, https://doi.org/10.12991/marupj.300322. -243.

[31] C.G. Mortimer, G. Wells, J.P. Crochard, E.L. Stone, T.D. Bradshaw, M.F. Stevens, A. D. Westwell, Antitumor benzothiazoles. 26.(1) 2-(3,4-dimethoxyphenyl)-5-fluorobenzothiazole (GW 610, NSC 721648), a simple fluorinated 2-arylbenzothiazole, shows potent and selective inhibitory activity against lung, colon, and breast cancer cell lines, J. Med. Chem. 49 (2006) 179–185, https://doi.org/10.1021/jm050942k.

[32] L. Racane, S.K. Pavelic, R. Nhili, S. Depauw, C. Paul-Constant, I. Ratkaj, M. H. David-Cordonnier, K. Pavelic, V. Tralic-Kulenovic, G. Karminski-Zamola, New anticancer active and selective phenylene-bisbenzothiazoles: synthesis, antiproliferative evaluation and DNA binding, Eur. J. Med. Chem. 63 (2013) 882–891, https://doi.org/10.1016/j.ejmech.2013.02.026.

[33] R. Dubey, P.K. Shrivastava, P.K. Basniwal, S. Bhattacharya, N.S. Moorthy, 2-(4-aminophenyl) benzothiazole: a potent and selective pharmacophore with novel mechanistic action towards various tumour cell lines, Mini. Rev. Med. Chem. 6 (2006) 633–637, https://doi.org/10.2174/138955706777435706.

[34] O.A. Phillips, E.E. Udo, S.M. Samuel, Synthesis and structure-antibacterial activity of triazolyl oxazolidinones containing long chain acyl moiety, Eur. J. Med. Chem. 43 (2008) 1095–1104, https://doi.org/10.1016/j.ejmech.2007.07.006.

[35] W.J. Watkins, L. Chong, A. Cho, R. Hilgenkamp, M. Ludwikow, N. Garizi, N. Iqbal, J. Barnard, R. Singh, D. Madsen, K. Lolans, O. Lomovskaya, U. Oza, P. Kumaraswamy, A. Blecken, S. Bai, D.J. Loury, D.C. Griffith, M.N. Dudley, Quinazolinone fungal efflux pump inhibitors. Part 3: (N-methyl)piperazine variants and pharmacokinetic optimization, Bioorg. Med. Chem. Lett. 17 (2007) 2802–2806, https://doi.org/10.1016/j.bmcl.2007.02.047.

[36] L. Yu, X. Gan, D. Zhou, F. He, S. Zeng, D. Hu, Synthesis and Antiviral Activity of Novel 1,4-Pentadien-3-one Derivatives Containing a 1,3,4-Thiadiazole Moiety, Molecules. (2017) 22, https://doi.org/10.3390/molecules22040658.

[37] S. Bala, N. Sharma, A. Kajal, S. Kamboj, V. Saini, Mannich bases: an important pharmacophore in present scenario, Int. J. Med. Chem. (2014) 191072, https://doi.org/10.1155/2014/191072, 2014.

[38] O.M. Becker, D.S. Dhanoa, Y. Marantz, D. Chen, S. Shacham, S. Cheruku, A. Heifetz, P. Mohanty, M. Fichman, A. Sharadendu, R. Nudelman, M. Kauffman, S. Noiman, An integrated in silico 3D model-driven discovery of a novel, potent, and selective amidosulfonamide 5-HT1A agonist (PRX-00023) for the treatment of anxiety and depression, J. Med. Chem. 49 (2006) 3116–3135, https://doi.org/10.1021/jm0508641.

[39] N. Samie, S. Muniandy, M.S. Kanthimathi, B.S. Haerian, Mechanism of action of novel piperazine containing a toxicant against human liver cancer cells, PeerJ 4 (2016) e1588, https://doi.org/10.7717/peerj.1588.

[40] L. Akl, A.A. Abd El-Hafeez, T.M. Ibrahim, R. Salem, H.M.M. Marzouk, R.A. El-Domany, P. Ghosh, W.M. Eldehna, S.M. Abou-Seri, Identification of novel piperazine-tethered phthalazines as selective CDK1 inhibitors endowed with *in vitro* anticancer activity toward the pancreatic cancer, Eur. J. Med. Chem. 243 (2022) 114704, https://doi.org/10.1016/j.ejmech.2022.114704.

[41] E.E. Gurdal, B. Turgutalp, H.O. Gulcan, T. Ercetin, M.F. Sahin, I. Durmaz, R. C. Atalay, Q.D. Nguyen, W. Sippl, M. Yarim, Synthesis of Novel Benzothiazole-Piperazine Derivatives and Their Biological Evaluation as Acetylcholinesterase

Inhibitors and Cytotoxic Agents, Anti-Cancer Agent Me 17 (2017) 1837–1845, https://doi.org/10.2174/1871520617666170412153604.
[42] Y. Ma, X. Zheng, H. Gao, C. Wan, G. Rao, Z. Mao, Design, Synthesis, and Biological Evaluation of Novel Benzofuran Derivatives Bearing N-Aryl Piperazine Moiety, Molecules. 21 (2016), https://doi.org/10.3390/molecules21121684.
[43] H.H. Lin, W.Y. Wu, S.L. Cao, J. Liao, L. Ma, M. Gao, Z.F. Li, X. Xu, Synthesis and antiproliferative evaluation of piperazine-1-carbothiohydrazide derivatives of indolin-2-one, Bioorg. Med. Chem. Lett. 23 (2013) 3304–3307, https://doi.org/10.1016/j.bmcl.2013.03.099.
[44] S.L. Cao, Y. Han, C.Z. Yuan, Y. Wang, Z.K. Xiahou, J. Liao, R.T. Gao, B.B. Mao, B. L. Zhao, Z.F. Li, X. Xu, Synthesis and antiproliferative activity of 4-substituted-piperazine-1-carbodithioate derivatives of 2,4-diaminoquinazoline, Eur. J. Med. Chem. 64 (2013) 401–409. 10.1016/j.ejmech.2013.04.017.
[45] A. Chopra, A. Anderson, C. Giardina, Novel piperazine-based compounds inhibit microtubule dynamics and sensitize colon cancer cells to tumor necrosis factor-induced apoptosis, J. Biol. Chem. 289 (2014) 2978–2991, https://doi.org/10.1074/jbc.M113.499319.
[46] L. Yurttas, Z.A. Kaplancikli, S. Gorgulu-Kahyaoglu, New N'-Arylidene-2-[(4-Nitrophenyl)Piperazın-1-yl]Acetohydrazide Derivatives: synthesis and Anticancer Activity Investigation, Lett. Drug Des. Discov. (2017) 14, https://doi.org/10.2174/1570180814666161207163450.
[47] L. Yurttas, S. Demirayak, S. Ilgin, O. Atli, *In vitro* antitumor activity evaluation of some 1,2,4-triazine derivatives bearing piperazine amide moiety against breast cancer cells, Bioorg. Med. Chem. 22 (2014) 6313–6323, https://doi.org/10.1016/j.bmc.2014.10.002.
[48] L. Yurttas, G.A. Ciftci, H.E. Temel, B.N. Saglik, B. Demir, S. Levent, Biological Activity Evaluation of Novel 1,2,4-Triazine Derivatives Containing Thiazole/Benzothiazole Rings, Anti-Cancer Agent Me 17 (2017) 1846–1853, https://doi.org/10.2174/1871520617666170327151031.
[49] A.E. Evren, L. Yurttaş, B. Ekselli, G. Akalın-Cıftcı, Novel Tri-substituted Thiazoles Bearing Piperazine Ring: synthesis and Evaluation of their Anticancer Activity, Lett. Drug Des. Discov. 16 (2019) 547–555, https://doi.org/10.2174/1570180815666180731122118.
[50] L. Yurttaş, A.E. Evren, A. Kubilay, H.E. Temel, Synthesis of New 1,2,4-Triazole Derivatives and Investigation of Their Matrix Metalloproteinase-9 (MMP-9) Inhibition Properties, Acta Pharmaceutica Sciencia 59 (2021) 216–232, https://doi.org/10.23893/1307-2080.aps.05913.
[51] A.E. Evren, L. Yurttaş, B. Ekselli, O. Aksoy, G. Akalin-Çiftçi, Design and Efficient Synthesis of Novel 4,5-Dimethylthiazole-Hydrazone Derivatives and their Anticancer Activity, Lett. Drug Des. Discov. 18 (2021) 372–386, https://doi.org/10.2174/1570180817999201022192937.
[52] S. Dawbaa, A.E. Evren, Z. Cantürk, L. Yurttaş, Synthesis of new thiazole derivatives and evaluation of their antimicrobial and cytotoxic activities, Phosphorus. Sulfur. Silicon. Relat. Elem. 196 (2021) 1093–1102, https://doi.org/10.1080/10426507.2021.1972299.
[53] A.E. Evren, D. Nuha, S. Dawbaa, B.N. Saglik, L. Yurttas, Synthesis of novel thiazolyl hydrazone derivatives as potent dual monoamine oxidase-aromatase inhibitors, Eur. J. Med. Chem. 229 (2022) 114097, https://doi.org/10.1016/j.ejmech.2021.114097.
[54] A.E. Evren, D. Nuha, L. Yurttaş, Focusing on the moderately active compound (MAC) in the design and development of strategies to optimize the apoptotic effect by molecular mechanics techniques, European Journal of Life Sciences 1 (2022) 118–126, https://doi.org/10.55971/ejls.1209591.
[55] O.M. Salih, M.A. Al-Sha'er, H.A. Basheer, Novel 2-Aminobenzothiazole Derivatives: docking, Synthesis, and Biological Evaluation as Anticancer Agents, ACS. Omega 9 (2024) 13928–13950, https://doi.org/10.1021/acsomega.3c09212.
[56] A. Amin, B.A. Bhat, Z. Ul-Khazir, A.A. Hurrah, I.A. Bhat, P.K. Sharma, K. Z. Masoodi, Benzothiazole-Piperazine Hybrids Effectively Target C4-2 Castration-Resistant Prostate Cancer Cells *in vitro* Implicated through Computational Studies, ChemistrySelect. 9 (2024) e202401401, https://doi.org/10.1002/slct.202401401.
[57] E.E. Gurdal, E. Buclulgan, I. Durmaz, R. Cetin-Atalay, M. Yarim, Synthesis and anticancer activity evaluation of some benzothiazole-piperazine derivatives, Anti-Cancer Agent Me, 15 (2015) 382–389. 10.2174/1871520615666141216151101.
[58] L. Yurttaş, A.E. Evren, A. Kubilay, M.O. Aksoy, H.E. Temel, G. Akalın Çiftçi, Synthesis of Some New 1,3,4-Oxadiazole Derivatives and Evaluation of Their Anticancer Activity, ACS. Omega (2023), https://doi.org/10.1021/acsomega.3c07776.
[59] M.D. Altintop, B. Sever, G. Akalin Ciftci, G. Turan-Zitouni, Z.A. Kaplancikli, A. Ozdemir, Design, synthesis, *in vitro* and in silico evaluation of a new series of oxadiazole-based anticancer agents as potential Akt and FAK inhibitors, Eur. J. Med. Chem. 155 (2018) 905–924, https://doi.org/10.1016/j.ejmech.2018.06.049.
[60] Y. Lu, H. Sun, Progress in the Development of Small Molecular Inhibitors of Focal Adhesion Kinase (FAK), J. Med. Chem. 63 (2020) 14382–14403, https://doi.org/10.1021/acs.jmedchem.0c01248.
[61] C.A. Lipinski, F. Lombardo, B.W. Dominy, P.J. Feeney, Experimental and computational approaches to estimate solubility and permeability in drug discovery and development settings, Adv. Drug Deliv. Rev. 23 (1997) 3–25, https://doi.org/10.1016/s0169-409x(96)00423-1.
[62] L. Yurttas, A.E. Evren, H. AlChaib, H.E. Temel, G. Akalin Ciftci, Synthesis, molecular docking, and molecular dynamic simulation studies of new 1,3,4-thiadiazole derivatives as potential apoptosis inducers in A549 lung cancer cell line, J. Biomol. Struct. Dyn. (2024) 1–16, https://doi.org/10.1080/07391102.2023.2300125.
[63] D. Nuha, A.E. Evren, Ö. Kapusiz, Ü.D. Gül, N. Gundogdu-Karaburun, A. Ç. Karaburun, H. Berber, Design, synthesis, and antimicrobial activity of novel coumarin derivatives: an in-silico and in-vitro study, J. Mol. Struct. 1272 (2023) 134166, https://doi.org/10.1016/j.molstruc.2022.134166.
[64] S.A. Naji, B.N. Sağlik, M. Agamennone, A.E. Evren, N. Gundogdu-Karaburun, A. Ç. Karaburun, Design and Evaluation of Synthesized Pyrrole Derivatives as Dual COX-1 and COX-2 Inhibitors Using FB-QSAR Approach, ACS. Omega (2023), https://doi.org/10.1021/acsomega.3c06344.
[65] D. Osmaniye, A.E. Evren, B.N. Saglik, S. Levent, Y. Ozkay, Z.A. Kaplancikli, Design, synthesis, biological activity, molecular docking, and molecular dynamics of novel benzimidazole derivatives as potential AChE/MAO-B dual inhibitors, Arch. Pharm. (Weinheim) 355 (2022) e2100450, https://doi.org/10.1002/ardp.202100450.
[66] N.T. Yucel, A.A.R. Asfour, A.E. Evren, C. Yazici, U. Kandemir, U.D. Ozkay, O. D. Can, L. Yurttas, Design and synthesis of novel dithiazole carboxylic acid Derivatives: *in vivo* and in silico investigation of their Anti-Inflammatory and analgesic effects, Bioorg. Chem. 144 (2024) 107120, https://doi.org/10.1016/j.bioorg.2024.107120.
[67] A.Z. Kaya, D. Osmaniye, A.E. Evren, L. Yurttaş, Ş. Demirayak, Synthesis, Cytotoxic Activity Evaluation and Molecular Docking Studies of Some Benzimidazole Derivatives, Cumhuriyet Science Journal 45 (2024) 80–87, https://doi.org/10.17776/csj.1392037.
[68] S. Dawbaa, C. Turkes, D. Nuha, Y. Demir, A.E. Evren, L. Yurttas, S. Beydemir, New N-(1,3,4-thiadiazole-2-yl)acetamide derivatives as human carbonic anhydrase I and II and acetylcholinesterase inhibitors, J. Biomol. Struct. Dyn. (2024) 1–19, https://doi.org/10.1080/07391102.2024.2331085.
[69] S. Krautwald, E. Ziegler, L. Rolver, A. Linkermann, K.A. Keyser, P. Steen, K. C. Wollert, M. Korf-Klingebiel, U. Kunzendorf, Effective blockage of both the extrinsic and intrinsic pathways of apoptosis in mice by TAT-crmA, J. Biol. Chem. 285 (2010) 19997–20005, https://doi.org/10.1074/jbc.M110.122127.
[70] L. Yurttaş, A.E. Evren, A. Kubilay, H.E. Temel, G.A. Çiftçi, 3,4,5-Trisubstituted-1,2,4-triazole Derivatives as Antiproliferative Agents: synthesis, *In vitro* Evaluation and Molecular Modelling, Lett. Drug Des. Discov. 17 (2020) 1502–1515, https://doi.org/10.2174/1570180817999200712190831.
[71] A.E. Evren, L. Yurttas, B. Ekselli, G. Akalin-Ciftci, Synthesis and biological evaluation of 5-methyl-4-phenyl thiazole derivatives as anticancer agents, Phosphorus. Sulfur. Silicon. Relat. Elem. 194 (2019) 820–828, https://doi.org/10.1080/10426507.2018.1550642.
[72] D. Nuha, A.E. Evren, Z.S. Ciyanci, H.E. Temel, G. Akalin Ciftci, L. Yurttas, Synthesis, density functional theory calculation, molecular docking studies, and evaluation of novel 5-nitrothiophene derivatives for anticancer activity, Arch. Pharm. (Weinheim) 355 (2022) e2200105, https://doi.org/10.1002/ardp.202200105.
[73] T. Mosmann, Rapid colorimetric assay for cellular growth and survival: application to proliferation and cytotoxicity assays, J. Immunol. Methods 65 (1983) 55–63, https://doi.org/10.1016/0022-1759(83)90303-4.
[74] K. Keiser, C.C. Johnson, D.A. Tipton, Cytotoxicity of mineral trioxide aggregate using human periodontal ligament fibroblasts, J. Endod. 26 (2000) 288–291.
[75] L. Yurttas, B. Demir, G.A. Ciftci, Some Thiazole Derivatives Combined with Different Heterocycles: cytotoxicity Evaluation and Apoptosis Inducing Studies, Anti-Cancer Agent Me, 18 (2018) 1115–1121. 10.2174/1871520618666180328115314.
[76] G.A. Ciftci, A. Iscan, M. Kutlu, Escin reduces cell proliferation and induces apoptosis on glioma and lung adenocarcinoma cell lines, Cytotechnology 67 (2015) 893–904, https://doi.org/10.1007/s10616-015-9877-6.
[77] L. Yurttas, Y. Ozkay, G. Akalin-Ciftci, S. Ulusoylar-Yildirim, Synthesis and anticancer activity evaluation of N-[4-(2-methylthiazol-4-yl)phenyl]acetamide derivatives containing (benz)azole moiety, J Enzyme Inhib Med Ch 29 (2014) 175–184, https://doi.org/10.3109/14756366.2013.763253.
[78] N.P. Kumar, P. Sharma, T.S. Reddy, N. Shankaraiah, S.K. Bhargava, A. Kamal, Microwave-assisted one-pot synthesis of new phenanthrene fused-tetrahydrodibenzo-acridinones as potential cytotoxic and apoptosis inducing agents, Eur. J. Med. Chem. 151 (2018) 173–185, https://doi.org/10.1016/j.ejmech.2018.03.069.
[79] L.R. de Souza Neto, J.T. Moreira-Filho, B.J. Neves, R. Maidana, A.C.R. Guimaraes, N. Furnham, C.H. Andrade, F.P. Silva Jr., In silico Strategies to Support Fragment-to-Lead Optimization in Drug Discovery, Front. Chem. 8 (2020) 93, https://doi.org/10.3389/fchem.2020.00093.
[80] T.I. Adelusi, A.-Q.K. Oyedele, I.D. Boyenle, A.T. Ogunlana, R.O. Adeyemi, C. D. Ukachi, M.O. Idris, O.T. Olaoba, I.O. Adedotun, O.E. Kolawole, Y. Xiaoxing, M. Abdul-Hammed, Molecular modeling in drug discovery, Inform. Med. Unlocked. 29 (2022) 100880, https://doi.org/10.1016/j.imu.2022.100880.
[81] R. Han, H. Yoon, G. Kim, H. Lee, Y. Lee, Revolutionizing Medicinal Chemistry: the Application of Artificial Intelligence (AI) in Early Drug Discovery, Pharmaceuticals. (Basel) 16 (2023), https://doi.org/10.3390/ph16091259.
[82] Molinspiration, Calculation of Molecular Properties and Bioactivity Score.
[83] Molsoft, Drug-likeness and Molecular Property Prediction.
[84] A. Daina, O. Michielin, V. Zoete, SwissADME: a free web tool to evaluate pharmacokinetics, drug-likeness and medicinal chemistry friendliness of small molecules, Sci. Rep. 7 (2017) 42717, https://doi.org/10.1038/srep42717.
[85] J. Walters, J.L. Schipper, P. Swartz, C. Mattos, A.C. Clark, Allosteric modulation of caspase 3 through mutagenesis, Biosci. Rep. 32 (2012) 401–411, https://doi.org/10.1042/BSR20120037.
[86] C. Cade, P. Swartz, S.H. MacKenzie, A.C. Clark, Modifying caspase-3 activity by altering allosteric networks, Biochemistry 53 (2014) 7582–7595, https://doi.org/10.1021/bi500874k.
[87] S. Maestro, Version 10.6, LLC, New York, 2016.
[88] QikProp, Version 4.8, Schrödinger, LLC, New York, NY, 2016.

[89] A.E. Evren, D. Nuha, S. Dawbaa, A.B. Karaduman, B.N. Saglik, L. Yurttas, Novel oxadiazole-thiadiazole derivatives: synthesis, biological evaluation, and in silico studies, J. Biomol. Struct. Dyn. (2023) 1–13, https://doi.org/10.1080/07391102.2023.2247087.

[90] B.N. Saglik, A.M. Sen, A.E. Evren, U.A. Cevik, D. Osmaniye, B. Kaya Cavusoglu, S. Levent, A.B. Karaduman, Y. Ozkay, Z.A. Kaplancikli, Synthesis, investigation of biological effects and in silico studies of new benzimidazole derivatives as aromatase inhibitors, Z. Naturforsch. C. J. Biosci. 75 (2020) 353–362, https://doi.org/10.1515/znc-2020-0104.

[91] D. Osmaniye, A.E. Evren, Ş. Karaca, Y. Özkay, Z.A. Kaplancıklı, Novel thiadiazol derivatives; design, synthesis, biological activity, molecular docking and molecular dynamics, J. Mol. Struct. 1272 (2023) 134171, https://doi.org/10.1016/j.molstruc.2022.134171.

[92] A.E. Evren, A.B. Karaduman, B.N. Saglik, Y. Ozkay, L. Yurttas, Investigation of Novel Quinoline-Thiazole Derivatives as Antimicrobial Agents: in Vitro and In Silico Approaches, ACS. Omega 8 (2023) 1410–1429, https://doi.org/10.1021/acsomega.2c06871.

[93] A.A. Al-Sharabi, A.E. Evren, B.N. Saglik, L. Yurttas, Synthesis, characterization, molecular docking and molecular dynamics simulations of novel 2,5-disubstituted-1,3,4-thiadiazole derivatives as potential cholinesterase/monoamine oxidase dual inhibitors for Alzheimer's disease, J. Biomol. Struct. Dyn. (2023) 1–19, https://doi.org/10.1080/07391102.2023.2274967.

[94] D. Nuha, A.E. Evren, B.N.S. Ozkan, N. Gundogdu-Karaburun, A.C. Karaburun, Design, synthesis, biological evaluation, and molecular modeling simulations of new phthalazine-1,4-dione derivatives as anti-Alzheimer's agents, Arch. Pharm. (Weinheim) (2024) e2400067, https://doi.org/10.1002/ardp.202400067.

[95] N.T. Yucel, D. Osmaniye, U. Kandemir, A.E. Evren, O.D. Can, U.Demir Ozkay, Synthesis and Antinociceptive Effect of Some Thiazole-Piperazine Derivatives: involvement of Opioidergic System in the Activity, Molecules. 26 (2021), https://doi.org/10.3390/molecules26113350.

[96] A.E. Evren, D. Nuha, B.N.S. Ozkan, C. Kahraman, E.M. Gonulalan, L. Yurttas, Design and synthesis of phenoxy methyl-oxadiazole compounds against Alzheimer's disease, Arch. Pharm. (Weinheim) (2024) e2400115, https://doi.org/10.1002/ardp.202400115.

[97] Schrödinger Release 2020-3, Desmond, Schrödinger, LLC, New York, NY, USA, 2020.